The ELD4-OsPRR95 module represses *OsMADS51* in regulating rice heading date

Xin Jin[1,#], Wen Li[2,#], Xinyue Zhang[1,#], Fu-Qing Wu[1], Yupeng Wang[1], Yimin Ling[1], Jie Wang[1], Zhiwei Li[1], Lizhuo Ma[1], Xin Liu[1], Minxi Wu[1], Limin Zhang[1], Xudong Zhu[1], Ming Yu[1], Qiyu Yang[1], Yulong Ren[1], Cailin Lei[1], Qibin Lin[1], Zhijun Cheng[1], Zhichao Zhao[1], Xiuping Guo[1], Xin Wang[1], Shirong Zhou[2,*], Shanshan Zhu[1,*], Jianmin Wan[1,2,*]

[1] State Key Laboratory of Crop Gene Resources and Breeding, National Key Facility for Crop Gene Resources and Genetic Improvement, Institute of Crop Sciences, Chinese Academy of Agricultural Sciences, Beijing 100081, China

[2] State Key Laboratory for Crop Genetics & Germplasm Enhancement and Utilization, Nanjing Agricultural University, Nanjing 210095, China

[#] These authors contributed equally to this work

* Address corresponding to Jianmin Wan, wanjianmin@caas.cn, Shanshan Zhu, zhushanshan@caas.cn and Shirong Zhou, srzhou@njau.edu.cn

Short title: ELD4-OsPRR95 regulates rice heading date

The authors responsible for distribution of materials integral to the findings presented in this article in accordance with the policy described in the Instructions for Authors (https://academic.oup.com/plcell/pages/General-Instructions) are: Jianmin Wan, wanjianmin@caas.cn, Shanshan Zhu, zhushanshan@caas.cn and Shirong Zhou, srzhou@njau.edu.cn

Abstract

Heading date is a key agronomic trait that affects crop yield and regional adaptability. In this study, we identified a rice (*Oryza sativa*) early heading mutant and cloned the causal heading inhibitor gene *EARLY HEADING AT LONG DAY 4* (*ELD4*) using the MutMap method. The *eld4* CRISPR mutants and *ELD4* RNAi plants flowered earlier than the wild type under natural long-

day (NLD) conditions. ELD4 is a zinc finger transcription factor that localizes in the nucleus. Biochemical and genetic evidence suggests that ELD4 physically interacts with the pseudo-response regulator (PRR) protein OsPRR95. The *Osprr95* mutant also exhibits an earlier heading phenotype under NLD. ELD4 and OsPRR95 co-regulate heading date by directly binding to the promoter and the first intron of *OsMADS51*, which promotes heading date. Moreover, electrophoretic mobility shift and luciferase complementation assays showed that ELD4 enhances OsPRR95 binding to the first intron of *OsMADS51*. These results suggest that the ELD4-OsPRR95 module directly represses *OsMADS51* in regulating flowering time. Haplotype analysis reveals that *OsPRR95* haplotype 3, which is geographically distributed in the north, exhibits a shorter heading date than haplotype 1 found in the south. This indicates that selection at the *OsPRR95* locus has enhanced the regional adaptability of rice.

Introduction

Rice, a facultative short-day plant, exhibits earlier flowering under short-day (SD) conditions and delayed flowering under long-day (LD) conditions (Zhang et al. 2019). Flowering is an important event in the whole life of plants. Appropriate flowering time is a crucial process in determining plant production. The heading date is an important agronomic trait, which determines crop yield and regional adaptability (Xu et al. 2022; Wang et al. 2019; Cai et al. 2021). The flowering of plants is a complex and delicate process, influenced by various internal and external factors such as temperature, photoperiod, and hormones, among which the photoperiod is the most significant factor and also the most extensively studied (Zhang et al. 2019; Song et al. 2013).

The photoperiod regulation of rice heading date mainly includes two relatively conserved pathways. One is the *OsGI* (*GIGANTEA*)-*Hd1* (*Heading date 1*) -*Hd3a* (*Heading date 3a*) pathway. In which *OsGI* integrates signals and regulates the *Hd1* gene (Yano et al. 2000), the homologous gene of Arabidopsis *CONSTANS* (*CO*). *Hd1* acts as a flowering promoter under SD conditions by enhancing the expression of the florigen gene *Hd3a*, while it functions as a flowering inhibitor under LD conditions by suppressing the expression of *RFT1* (Yano et al. 2000; Kojima et al. 2002; Hayama et al. 2003; Tamaki et al. 2007). In addition to the conserved pathways, rice has a unique photoperiodic pathway for controlling flowering: the *Ehd1* (*Early heading date 1*)-*RFT1 (RICE FLOWERING LOCUS T1)/Hd3a* pathway. *Ehd1* is an important integrator of heading date regulatory network in rice, encoding a B-type response regulator

protein that includes a GARP domain, which is crucial for its DNA-binding ability (Doi et al. 2004). *Ehd1* promotes rice flowering by inducing the expression of *RFT1* and *Hd3a* independently of *Hd1* under SD conditions, while *Ehd1* can also promote rice flowering even when *Hd1* inhibits the heading under LD conditions (Doi et al. 2004). Many regulators of *Ehd1* have been identified which include *Ghd7* (*Grain number, plant height and heading date 7*) (Xue et al. 2008), *DTH8* (*Days to heading 8*) (Yan et al. 2011), *OsPRR37* (*Oryza sativa Pseudo-Response Regulator 37*) (Koo et al. 2013) and *OsMADS51* (Kim et al. 2007) etc. *OsMADS51,* an upstream regulator of *Ehd1*, is a key promoter of heading date (Kim et al. 2007). Previous studies have demonstrated that *OsMADS51* is the functional gene underlying *qHd1* (Chen et al. 2018). The presence or absence of a 9.5-kb insertion in the first intron of *OsMADS51* has been shown to regulate the thermosensitive-mediated heading date in rice (Chen et al. 2018). Above studies suggest that *OsMADS51* is an important gene mediating rice heading date. However, the direct upstream regulator of *OsMADS51* has not yet been reported. BBX (B-Box) is a subfamily of the zinc finger protein family, which contains one or two highly conserved B-Box domains at N-terminus of the amino acid sequences that can bind to zinc ions and participate in protein-protein interactions (Klug et al. 1995). And Some BBX proteins also include the CCT domain (Khanna et al. 2009). BBX proteins are divided into five types based on the number of B-Box domains and the presence or absence of the CCT domain (Klug et al. 1995; Huang et al. 2012). In addition to the B-Box and CCT domains, some BBX proteins have a six-amino acid sequence composed of valine and proline located approximately 16 to 20 amino acid residues upstream of their CCT domain (Gangappa et al. 2014; Datta et al. 2006; Holm et al. 2001). BBX proteins are widely present in eukaryotic organisms. There are 32 BBX proteins in Arabidopsis (Khanna et al. 2009) and 30 BBX proteins in rice (Huang et al. 2012). These BBX proteins in plants have been reported to play important roles in photomorphogenesis, stress response and hormone signal transduction. *BBX4, BBX20, BBX21, BBX22, BBX24, BBX25, BBX32* play a crucial role in regulating hypocotyl elongation in Arabidopsis (Datta et al. 2006; Fan et al. 2012; Datta et al. 2007; Datta et al. 2008; Gangappa et al. 2013; Holtan et al. 2011; Kumagai et al. 2008). *BBX18* and *BBX19* are involved in the regulation of de-etiolation in Arabidopsis seedlings (Khanna et al. 2006). BBX proteins also participate in the regulation of plant stress responses, including high temperature, low temperature, and salt stress, such as BBX18 being involved in the regulation of

Arabidopsis tolerance to high temperature (Wang et al. 2013); BBX24 is involved in the regulation of Arabidopsis salt stress tolerance (Nagaoka et al. 2003).

The Pseudo-Response Regulator (PRR) family proteins, including TOC1 (also known as PRR1), PRR3, PRR5, PRR7, and PRR9 in *Arabidopsis*, are core components of the circadian clock (Matsushika et al. 2000; Nakamichi et al. 2010). PRRs contain Pseudo Receiver (PR) and CCT motifs (Nakamichi et al. 2010). They are typically reported as transcriptional repressors involved in regulating the circadian clock and flowering time (Nakamichi et al. 2010; Li et al. 2021; Nakamichi et al. 2005; Fornara et al. 2009; Yang et al. 2021). In addition, PRR proteins also play crucial roles in regulating the flowering of many crops, such as *Ppd-H1* in barley, *Ppd-D1a* and *TaPRR95* in wheat, *GmPRR37* in soybean and *PRR37* in sorghum (Turner et al. 2005; Beales et al. 2007; Fu et al. 2024; Wang et al. 2020; Murphy et al. 2011). There are five PRR members in rice: *OsPRR1, OsPRR37, OsPRR59, OsPRR73,* and *OsPRR95* (Murakami et al. 2007). *OsPRR37/DTH7* regulates heading in response to photoperiod and contributes to the regional adaptation in rice (Koo et al. 2013; Gao et al. 2014; Liu et al. 2018; Hu et al. 2021), while *OsPRR59* inhibits flowering time by repressing expression of *Ehd3* (Wang et al. 2022). In rice, *OsPRR95* has been documented to modulate the interplay among the circadian clock, photosynthesis, and abscisic acid (ABA) response pathways (Wang et al. 2022; Chen et al. 2022). However, the action mode of *OsPRR95* in heading date is currently not well understood. Further investigation for the function of OsPRR95 is warranted to elucidate the complex regulatory networks underlying heading date in rice.

In this study, we identified three early heading mutants under long-day conditions from screening an ethyl methanesulfonate (EMS)-induced mutagenesis mutant population, and cloned *ELD4* using the modified MutMap method. *ELD4* encodes a BBX family zinc finger transcription factor that is localized in the nucleus. Further studies revealed that ELD4 interacts with OsPRR95, a transcription regulator containing PR and CCT motifs. Genetic and molecular studies revealed that OsPRR95 shares a similar function with ELD4, and acts in the same pathway in regulating rice heading. Additionally, it was discovered that ELD4 enhances the binding of OsPRR95 to the first intron of *OsMADS51*, thereby directly regulating its expression. Haplotype analysis revealed that *OsPRR95* haplotype 3 (Hap 3), predominantly distributed in the north, exhibits a shorter heading date than haplotype 1 (Hap 1) from the south. This suggests that

selection at the *OsPRR95* locus has enhanced regional adaptability of rice during evolution. We demonstrate that ELD4 functions as a negative regulator of heading date in rice by promoting the binding of its interacting protein OsPRR95 to the expression of *OsMADS51*. Additionally, the geographical distribution of different *OsPRR95* haplotypes indicates that *OsPRR95* may represent a novel genetic resource for modulating regional adaptation in rice.

Result

1. Identification of *Early Heading at Long Day 4* through MutMap

To identify novel regulators of heading date, mutants with abnormal heading were screened from an EMS-mutagenized population in the japonica cultivar Ningjing 7 (NJ7). Among them, *eld4-1* flowered about 10 days earlier under natural long-day (NLD) conditions (Fig. 1A, B). An F_2 population derived from a cross between *eld4-1* and NJ7 showed a segregation ratio of early to normal heading close to 1:3 under NLD (Supplementary Table 1), indicating that the early-heading phenotype is controlled by a single recessive gene.

Using a modified MutMap (Abe et al. 2012) strategy with 30 early- and 30 normal-heading F_2 plants, *ELD4* was mapped to the distal end of chromosome 9 (Fig. 1C). Analysis of high-confidence SNPs and Sanger sequencing identified a C-to-A mutation in the second exon of *LOC_Os09g35880* in *eld4-1*, resulting in a histidine-to-glutamine substitution at position 42 of the encoded B-box zinc finger protein (Fig. 1D).

Two additional mutants, *eld4-2* and *eld4-3*, exhibiting similar early-heading phenotypes (10–13 days), were identified from the same mutagenesis library (Supplementary Fig. 1A, 1B, 1E, 1F). MutMap located their causal mutations to the same region as *eld4-1* (Supplementary Fig. 1C, 1G). Sequencing revealed amino acid changes in *LOC_Os09g35880*: arginine to lysine at position 93 in *eld4-2*, and cysteine to tyrosine at position 59 in *eld4-3* (Supplementary Fig. 1D, 1H). The consistent phenotypes and mutations in the same gene confirm that the mutation of *LOC_Os09g35880* is responsible for the phenotype of *eld4*. Additionally, amino acid sequence conservative analysis among different species shows that the mutated 42nd histidine, 59th cysteine and 93rd arginine are highly conserved among different species (Supplementary Fig. 2), underscoring its functional importance.

2. ELD4 negatively regulates heading date in rice

To further validate the role of *ELD4*, CRISPR/Cas9 system was used to generate knockout mutants in *japonica* cultivars Nipponbare (NIP) and Asominari (Aso). Two sgRNAs targeting the third exon of *ELD4* produced homozygous mutants with frameshift-induced premature termination (*eld4-4* and *eld4-5* in NIP, *eld4-6* and *eld4-7* in Aso) (Supplementary Fig. 3; Fig. 1I). All mutants showed earlier heading about 6 days under NLD (Fig. 1E, 1H, 1J, 1K).

RNAi knockdown lines targeting *ELD4* in NIP (*ELD4RNAi-2* and *ELD4RNAi-4*) with reduced *ELD4* expression (Supplementary Fig. 4) also headed about 5 days earlier under NLD (Fig. 1L, 1M). Conversely, overexpression lines (*OE-ELD4-1* and *OE-ELD4-2*) with elevated *ELD4* expression (Fig. 1G) showed delayed heading under NLD (Fig. 1F, 1H). These results confirm that ELD4 acts as a repressor of rice heading under long-day conditions.

To assess the impact of *ELD4* knockout mutants on yield, agronomic traits were evaluated. Compared to WT, *eld4* mutants showed significantly reduced grain number per plant and primary branches per panicle, but increased fertility. Plant height, tiller number, and secondary branches per panicle did not differ significantly (Supplementary Table 2).

3. ELD4 is a zinc finger transcription factor localized in the nucleus

Sequence analysis showed that ELD4 is a zinc finger transcription factor which has two B-BOX domains (Supplementary Fig. 5). To detect the temporal and spatial expression pattern of *ELD4*, reverse transcriptase-quantitative PCR (RT-qPCR) was performed to examine the relative expression of *ELD4* in different tissues. *ELD4* was constitutively expressed in all tissues with higher expression in the panicles and leaves (Fig. 2A). Meanwhile, we found that *ELD4* showed rhythmic expression patterns under both LD and SD conditions, which its expression gradually increases at ZT20, reaching a peak at ZT4, and then gradually decreases, reaching the lowest peak at ZT16 (Fig. 2B, 2C).

To examine the subcellular localization of ELD4 protein, an ELD4-GFP fusion vector with the control of the cauliflower mosaic virus 35S promoter (35S::ELD4-GFP) was constructed. The

construct was transformed into rice protoplasts, and the signal of ELD4-GFP fusion protein was found in the cytoplasm and nuclear which was merged with the signal of nuclear protein marker D53-mCherry (Zhou et al. 2013) fluorescence (Fig. 2D).

4. ELD4 physically interacts with OsPRR95

To investigate functional mode of ELD4, a yeast two-hybrid library (Y2H) screening assay was performed using pGBKT7-ELD4 as bait. A potential interacting protein, Pseudo-Response Regulator 95 (OsPRR95, LOC_Os09g36220), was identified. To confirm the interaction between ELD4 and OsPRR95, the full-length coding sequence (CDS) of *ELD4* was fused to pGADT7, while the full-length CDS of *OsPRR95* was fused to pGBKT7. Y2H assays showed that ELD4 can physically interact with OsPRR95 in yeast (Fig. 3A). An *in vitro* pull-down assay was also performed to verify the interaction. ELD4 was co-immunoprecipitated by OsPRR95-MBP, suggesting ELD4 physically interacts with OsPRR95 (Fig. 3C).

To further confirm the interaction *in planta*, a bimolecular fluorescence complementation (BiFC) assay in tobacco (*Nicotiana benthamiana*) leaves was performed. The signal of ELD4-cYFP and OsPRR95-nYFP combination was detected, but not detected in the controls (Fig. 3B). Additionally, the interaction between ELD4 and OsPRR95 was verified by split-luciferase complementation imaging (LCI) assays (Fig. 3D).

5. The genetic relationship between *ELD4* and *OsPRR95* in regulation of heading date

OsPRR95 was previously reported to regulate circadian rhythm and abscisic acid signaling in rice (Wang et al. 2022). To investigate whether *OsPRR95* regulates heading date, *Osprr95* mutants were generated using the CRISPR/Cas9 system. Two homozygous *Osprr95* mutants (*Osprr95-1* and *Osprr95-2*) in NIP background were identified, and both flowered earlier 3-4 days than WT under NLD condition (Fig. 4A, 4B and Supplementary Fig. 6). *OsPRR95* was also knocked out in the Zhonghua 11 (ZH11) background. Two homozygous *Osprr95* mutants (*Osprr95-3* and *Osprr95-4*) were obtained, and both exhibited a 4-5 days early flowering phenotype compared to the ZH11 under NLD conditions (Fig. 4C, 4D and 4E). Additionally,

OsPRR95 was overexpressed in ZH11. Two homozygous lines exhibiting increased expression showed 17-19 days delayed flowering phenotype under NLD conditions (Fig. 4F, 4G, 4H). These results suggested OsPRR95 negatively regulates rice heading date, similar with *ELD4*.

To investigate whether *ELD4* and *OsPRR95* function in the same pathway of heading date, an *eld4 Osprr95* double mutant was generated by crossing *eld4-4* with *Osprr95-1*. The *eld4 Osprr95* double mutant also displayed an early flowering phenotype under NLD conditions (Fig. 4I, 4J). In addition, to further check the potential epistatic relationship of *ELD4* and *OsPRR95* in genetics, we crossed *Osprr95-1* with the *OE-ELD4* over-expression line and obtained the *OE-ELD4 Osprr95* transgenic lines. Phenotypic analysis showed that *OE-ELD4 Osprr95* plants headed as early as the *osprr95* mutant, whereas *OE-ELD4* alone caused late heading (Supplementary Fig. 7). These results indicated that *ELD4* and *OsPRR95* function in the same pathway to regulate heading date and *OsPRR95* is epistatic to *ELD4* in genetics.

6. OsPRR95 interacts with itself and exhibits transcriptional repressive activity

To further characterize the function of OsPRR95, we analyzed the expression pattern and localization of OsPRR95. RT-qPCR analysis showed that *OsPRR95* is ubiquitously expressed in all rice tissues with higher expression level in sheath, panicle and leaves (Fig. 5A) and displays rhythmic expression patterns under both LD and SD conditions, which its expression gradually increases at ZT0, reaches a peak between ZT12, and then gradually decreases afterwards, reaching the lowest peak at ZT16 and ZT20. (Fig. 5B, 5C). Subcellular localization analysis in rice protoplasts shows that the OsPRR95-GFP fusion protein is localized in the nucleus and cytoplasm, co-localizing with the nuclear-localized D53-mCherry fusion protein (mCherry) (Fig. 5D).

Moreover, transcriptional activity assay demonstrated that OsPRR95 exhibits transcriptional repressive activity in rice protoplasts (Fig. 5E, 5F). In addition, OsPRR95 can interact with itself in yeast two-hybrid assays (Fig. 5G). To further confirm this interaction, LCI and BiFC assays were performed. The results showed that OsPRR95-cLUC interacted with OsPRR95-nLUC, and OsPRR95-cYFP interacted with OsPRR95-nYFP (Fig. 5H, 5I).

7. Both ELD4 and OsPRR95 bind to the promoter and the first intron of *OsMADS51*

To investigate the impact of *ELD4* on flowering-related genes, the expression levels of key flowering genes including *Ehd1*, *RFT1*, *Hd1*, *DTH8*, *OsMADS14*, *OsMADS50*, *OsGI, OsCOL4* and *OsTrx1* were analyzed in both the WT and *eld4-4* mutant under LD conditions. It was found that the expression levels of *RFT1*, *OsMADS14*, *OsGI* and *OsTrx1 genes* were significantly higher in the *eld4-4* mutant under LD conditions, while *Ehd1*, *Hd1*, *OsMADS50* and *OsCOL4 genes* under LD conditions were down-regulated in *eld4-4* mutant (Supplementary Fig. 8).

To further investigate the direct target genes regulated by ELD4, chromatin immunoprecipitation followed by sequencing (ChIP-seq) analysis was performed. Leaves from *ELD4* overexpressing lines were used for ChIP-seq analysis to investigate the genome-wide binding targets of ELD4. In total, 97 and 5550 significant peaks were identified in two replicates (Supplementary Data Set 1). These potential binding sites are primarily enriched within 3 kb of the Transcription Start Site (TSS) (Supplementary Fig. 9A). Notably, a ChIP-seq peak was identified on the first intron of *OsMADS51* in the ChIP-seq (Supplementary Fig. 9B). Consistent with this, the expression of *OsMADS51* was upregulated in both *eld4-5* and *Osprr95-1* mutants compared to WT (Supplementary Fig. 10A), suggesting that *OsMADS51* may be the direct target of ELD4. To verify binding of ELD4 to the first intron of *OsMADS51*, full-length *ELD4* was fused to the pB42AD vector, and the intron sequence of *OsMADS51* was cloned into the pLacZi vector (*OsMADS51*intro-pLacZi) for yeast one-hybrid assays. ELD4-AD can bind to *OsMADS51*intro-pLacZi, but not the control (Supplementary Fig. 10B, 10C), indicating that ELD4 can specifically bind to the first intron of *OsMADS51*.

Previous studies reported that OsPRR95 and BBX proteins binding regions are enriched with G-box containing motifs (Chen et al. 2022; Xu et al. 2016), and we discovered a potential G-box motif at 995 bp of *OsMADS51* promoter. To verify whether ELD4 binds to both the promoter and the first intron of *OsMADS51*, ChIP-qPCR assays using *ELD4* overexpression lines were performed. The results showed that ELD4 can bind to both the promoter and the first intron of *OsMADS51*, with a stronger binding to the intron (Fig. 6A, 6B). To further confirm whether ELD4 and OsPRR95 can directly bind to *OsMADS51*, electrophoretic mobility shift (EMSA) assays using both G-box and the first intron probe (named R-motif) were performed. The results demonstrated that there were very clear binding shift bands for both probes when ELD4 or

OsPRR95 protein was added (Fig. 6C, 6D). In addition, the shift bands were weakened when 50× and 250× competitive probes or a mutated probe were added (Fig. 6C, 6D).

In addition, the dual-luciferase reporter assays (Dual-LUC) were performed to further elucidate their interactions. The promoter or the first intron sequence of *OsMADS51* was fused to the firefly luciferase gene of the pGreen0800-LUC vector as the reporter (named *pOsMADS51*:LUC and *iOsMADS51*:LUC, respectively), and the CDS of *ELD4* and *OsPRR95* were individually inserted into pCAMBIA1390 vector as effectors, respectively. Then these fusion vectors were injected into tobacco leaves for the luciferase activity assay. When ELD4-Flag or OsPRR95-Flag was co-transformed with *pOsMADS51*:LUC reporter, no significant changes in luciferase activity were observed (Supplementary Fig. 11). However, when replaced the reporter *pOsMADS51*:LUC with the *iOsMADS51*:LUC, both ELD4 and OsPRR95 can inhibit the luciferase activity significantly (Fig. 6E, 6F). These results suggested that both ELD4 and OsPRR95 can bind to the promoter and the first intron probes of *OsMADS51*, with the first intron likely playing a dominant role.

To further investigate the biological consequence of ELD4-OsPRR95 module binding to the promoter and the intron region of *OsMADS51*, the EMSA assays were performed. Binding of OsPRR95 to the *OsMADS51* intron was enhanced with increasing amounts of ELD4-GST protein while declined with GST protein (Fig. 6G), indicating that ELD4 can enhance the binding of OsPRR95 to *OsMADS51* intron. To further verify this result, we performed the dual-luciferase reporter (Dual-LUC) assays in which the *iOsMADS51*:LUC construct was infiltrated alongside OsPRR95-Flag or ELD4-Flag at graded doses. Compared to the empty Flag vector, individual delivery of either OsPRR95-Flag or ELD4-Flag significantly attenuated LUC activity (Fig. 6H). When OsPRR95 and *iOsMADS51*:LUC were maintained at a fixed ratio, incremental elevation of co-expressed ELD4-Flag produced a dose-dependent reduction in LUC signal. Conversely, when ELD4-Flag and *iOsMADS51*:LUC were held constant, titration of OsPRR95-Flag elicited no additional change in luminescence (Fig. 6H).

8. ELD4 regulates the heading date of rice upstream of *OsMADS51*

To verify the genetic relationship between *ELD4* and *OsMADS51*, *OsMADS51* overexpressing transgenic lines (*OE-OsMADS51*) and *ELD4 OsMADS51* double overexpression lines (*OE-ELD4 OsMADS51*) driven by the maize ubiquitin promoter were generated in NIP background. Plants exhibiting upregulated expression were selected for flowering phenotype assessment (Supplementary Fig. 12). It was observed that the *OE-OsMADS51* overexpression plants flowered earlier, the *OE-ELD4* overexpression lines flowered later, while the *OE-ELD4 OsMADS51* double overexpression lines headed earlier (Fig. 6I, 6J), indicating that *OsMADS51* acts downstream of ELD4 to regulate flowering in rice.

To further confirm this conclusion, we generated the *osmads51* mutant by CRISPR/Cas9 (Supplementary Fig. 13A) and *eld4 osmads51* double mutant by crossing *osmads51* with *eld4* mutant. Phenotypic analysis of heading date in WT, *eld4*, *osmads51*, and *eld4 osmads51* revealed that *osmads51* exhibited a slightly delayed flowering time compared to WT, whereas *eld4* displayed a significantly early-heading phenotype. Notably, the *eld4 osmads51* double mutant only partially restored the early-heading phenotype of *eld4* (Supplementary Fig. 13B, 13C). These data indicated that *OsMADS51* acts downstream of ELD4 in regulating rice heading date and there may be additional downstream genes of ELD4 contributing to heading date regulation.

9. Natural variation of OsPRR95 suggests breeding selection among rice varieties

To elucidate the potential application value of *ELD4* and *OsPRR95*, haplotype analysis utilizing the RiceVarMap database (https://ricevarmap.ncpgr.cn/hap_net/) was performed. *ELD4* lacks haplotype differentiation in heading date, whereas *OsPRR95* exhibits such differentiation. Thus, we further analyze the haplotypes of *OsPRR95* involved in heading date determination. Four major haplotypes associated with the heading date at *OsPRR95* locus were identified (Fig. 7A). Detailed analysis of heading date phenotypes across these haplotypes revealed significant differences (Fig. 7B, 7C). Specifically, Hap 1 and Hap 2 exhibited longer heading period compared to Hap 3 and Hap 4 (Fig. 7B). This suggests that these four haplotypes may have distinct roles in the regulation of heading date in rice. To gain further insights into the genetic diversity and potential breeding applications, the distribution of rice varieties across the four haplotypes was examined. Analysis revealed that Hap 1 was predominantly found in *indica* rice varieties, while Hap 3 contained both *indica* and *japonica* varieties (Fig. 7D). Additionally, a

geographic distribution analysis of Hap 1 and Hap 3 was conducted (Fig. 7E). Hap 1 was found to be predominantly distributed in southern regions, while Hap 3 showed a more widespread distribution. However, there were no significant geographical distribution differences for Hap 2 and Hap 4. This geographic distribution pattern aligns with the observed differences in heading dates (Fig. 7B), as the longer heading date of Hap 1 is consistent with its adaptation to the longer growing seasons typically found in southern regions. Conversely, the shorter heading date of Hap 3 may confer an advantage in regions with shorter growing seasons or in environments where early maturation is beneficial. These results indicate that OsPRR95 is continuously selected in the evolutionary process, which enhances the regional adaptability of rice.

Discussion

In rice, the heading date is an important agronomic trait that determines the yield of crop and adaptability to different regions. In this study, we isolated a flowering-inhibitory gene *ELD4* from screening an ethyl methanesulfonate (EMS)-induced mutagenesis mutant population using the MutMap method (Fig. 1A-1D). ELD4 interacted with OsPRR95 to co-regulate the heading date in rice through binding to the promotor and the first intron of *OsMADS51* (Fig. 3, 4I, 4J and 6). Two genes with minor effects on the regulation of heading date were identified, which refines the regulatory network of heading date in rice. Concurrently, haplotype analysis of *OsPRR95* (Fig. 7) indicates that it has been subject to evolutionary selection, thereby enhancing the regional adaptability of rice breeding and cultivation.

It is noteworthy that all three mutants identified from the mutant population (*eld4-1, eld4-2,* and *eld4-3*) carry amino acid substitutions. Sequence alignment revealed that these altered residues are located within the B-Box domain and are conserved among members of the protein family (Supplementary Fig. 2), suggesting that they play crucial roles in protein function. Furthermore, structural modeling analysis using AlphaFold3 and PyMOL indicated that these amino acid substitutions likely disrupt the binding of ELD4 to the G-box motif in the *OsMADS51* promoter (Supplementary Fig. 14), also implying that *eld4-1*, *eld4-2*, and *eld4-3* are the loss-of-function mutants. This notion is further supported by the observation that these mutants exhibit heading phenotypes similar to those of the premature termination mutants (*eld4-4, eld4-5, eld4-6,* and *eld4-7* obtained by CRISPR/Cas9).

Previous studies have demonstrated that BBX19 and BBX28/29 interact with PRR proteins to modulate the circadian clock pathway (Li et al. 2021; Yu et al. 2023). Additionally, Hd1 has been shown to interact with OsPRR37 to regulate heading date in rice (Sun et al. 2022). However, the functional overlap and regulatory mechanisms of BBX and PRR family members in rice remain unclear. In this study, we found that ELD4 and OsPRR95 co-regulate heading date by binding to the promoter and intron of *OsMADS51* (Fig. 6A-6F), thereby refining the regulatory network underlying heading date in rice. Furthermore, recent evidence indicates that OsPRR95 is involved in ABA signaling during germination (Wang et al. 2022). Multiple BBX proteins have been reported to participate in abiotic stress responses (Wang et al. 2013; Nagaoka et al. 2003), the potential interaction between OsPRR95 and BBX proteins in mediating abiotic stress responses warrants further investigation.

Insertion of a 9.5-kb fragment into the first intron results in reduced transcription levels of *OsMADS51* and its downstream genes *Ehd1*, *Hd3a*, and *RFT1* under high-temperature conditions, thereby causing a delay in heading date, suggesting that *OsMADS51* is a key gene regulating rice heading date through temperature sensing pathway. (Zhao et al. 2024; Chen et al. 2018). In this study, the binding sites of ELD4 and OsPRR95 on *OsMADS51* were primarily located in the first intron, although binding to the promoter was also observed (Fig. 6A-6F). It is speculated whether *ELD4* and *OsPRR95* are also important genes regulating rice heading date via the temperature pathway, and the promoter and the first intron form a loop to repress gene expression in regulating the heading date of rice. The specific mechanism, as well as how high temperature affects this regulation requires further investigation.

Rice is a facultative short-day crop, which flowers earlier under SD conditions and delayed under LD conditions. In this study, the *Osprr95* mutant exhibited earlier heading under NLD conditions, while no significant change in heading date was observed compared to WT under NSD conditions (Fig. 4A-4C), indicating that *OsPRR95* is significantly affected by photoperiod. Previous study reported that the Evening complex (EC, containing ELF3 (EARLY FLOWERING 3), ELF4 (EARLY FLOWERING 4) and LUX (LUX ARRHYTHMO)) can integrate photoperiodic signals in rice. Under LD conditions, constitutively active *PhyB* suppresses ELF3.1 activity, thereby relieving the repression on downstream key flowering inhibitors (such as *OsPRR37*, *OsPRR95* and *Ghd7*). While, under SD conditions, low-activity

PhyB leads to the accumulation of the active form of ELF3-1, allowing EC to reduce the expression of these key flowering inhibitors (Andrade et al. 2022). Therefore, we propose that under SD conditions, the EC-mediated suppression of *OsPRR95* limits its activity, preventing the ELD4-OsPRR95 module from functioning, which makes the ELD4–OsPRR95 module operate specifically under LD conditions, not under SD conditions. However, the detailed mechanism still requires further investigation.

Integrating the above results, our study discovered an ELD4-OsPRR95 module regulating flowering time in rice. In WT, the OsPRR95 dimer interacts with ELD4 to jointly inhibit *OsMADS51* expression and delay rice flowering through inhibiting florigen. ELD4 also amplifies the repressive effect of OsPRR95 on *OsMADS51*. In *Osprr95* mutant, the absence of OsPRR95 protein mitigates the repression of *OsMADS51*, thereby releasing substantial amounts of *OsMADS51* and subsequently enhancing florigen production, which in turn advances the heading date in rice. In the *eld4* mutant, the downstream loss of ELD4 completely abolishes the repressive actions of both OsPRR95 and ELD4 on *OsMADS51*, leading to a more pronounced increase in florigen production and a significantly earlier heading date (Fig. 8). However, the phenotype of the double overexpression lines *OE-ELD4 OsMADS51* and *eld4 osmads51* double mutant suggested additional transcription factors or downstream genes may be involved in the regulation of heading date in rice through this pathway. RNA-seq analysis revealed that *Ghd2* (Grain number, plant height, and heading date 2) was significantly up-regulated in *eld4* compared with WT (Supplementary Fig. 15A). This observation was further validated by RT–qPCR, which showed that *Ghd2* expression was clearly up-regulated in *eld4*, *Osprr95*, and *eld4 Osprr95* mutants (Supplementary Fig. 15B). Moreover, we identified a G-box motif in the *Ghd2* promoter, and EMSA confirmed that ELD4 binds this G-Box motif (Supplementary Fig. 15C), indicating that *Ghd2* may also be a potential direct target of ELD4.

This study found that Hap 1, exhibiting a later heading date, is predominantly distributed in southern regions, whereas Hap 3, characterized by an earlier heading date, is more widely distributed in northern areas (Fig. 7). This distribution pattern is entirely consistent with regional adaptability. These results suggest that OsPRR95 has been under continuous evolutionary selection, likely driven by the need to adapt to varying photoperiodic and environmental conditions. The distinct haplotypes identified in this study may represent valuable genetic

resources for rice breeding, particularly in efforts to optimize heading date and enhance adaptability to different climatic zones. Future research could further explore the molecular mechanisms underlying the differences in heading date regulation among these haplotypes and investigate their potential applications in developing rice varieties with improved agronomic traits.

Materials and Methods

1. Growth conditions

The *eld4-1*, *eld4-2* and *eld4-3* mutants were identified from the ethyl methanesulfonate (EMS) mutagenesis in *japonica* rice variety Ningjing 7 (NJ7, wild type). For MutMap, NJ7 was crossed with *eld4-1*, *eld4-2* or *eld4-3* mutant, respectively. The F_1 plants were self-crossed to generate F_2 populations. For *eld4-4, eld4-5, eld4-6, eld4-7, Osprr95-1, Osprr95-2, Osprr95-3, Osprr95-4* and *osmads51* knockout plants, 20 bp gene-specific spacer sequences of *eld4-4, eld4-5, eld4-6, eld4-7, Osprr95-1, Osprr95-2, Osprr95-3, Osprr95-4* and *osmads51* were inserted into the sgRNA/Cas9 construct, respectively. For *ELD4RNAi-2* and *ELD4RNAi-4* transgenic plants, the 300bp coding sequence of *ELD4* was cloned into binary vector LH-FAD1390RNAi. For *OE-ELD4-1, OE-ELD4-2, OE-OsPRR95-2, OE-OsPRR95-3* and *OE-OsMADS51* overexpression constructs, full-length coding sequences of *ELD4, OsPRR95* and *OsMADS51* were cloned into binary vector pCAMBIA1390. Above constructs were introduced into Agrobacterium tumefaciens strain EHA105 and then transformed into the callus of the japonica cultivar variety, Nipponbare (*eld4-4, eld4-5, Osprr95-1, Osprr95-2, osmads51*, *ELD4RNAi-2, ELD4RNAi-4, OE-ELD4-1, OE-ELD4-2, OE-OsPRR95-2, OE-OsPRR95-3* and *OE-OsMADS51*), Aso (*eld4-6, eld4-7*), Zhonghua 11 (*Osprr95-3, Osprr95-4*). Data was obtained using T2-T5 generations for above plants. For MutMap, all plants were grown in the field of Nanjing. Plants for other assays were grown in the field of Beijing and Hainan during the natural growing season. For growth chambers treatments, all plants were grown under conditions of 10 h darkness, 25°C/14 h light, 30°C (LD) or 14 h darkness, 25°C/10 h light, 30°C (SD), light intensity of 500-800 $\mu mol \cdot m^{-2} \cdot s^{-1}$ and relative humidity of 70%. For field test, all plants were grown in the field of Shunyi, Beijing.

2. MutMap analysis

To isolate the mutated genes responsible for *eld4-1*, *eld4-2* and *eld4-3* phenotypes, F_2 population was constructed by crossing the *eld4-1*, *eld4-2* and *eld4-3* mutants with the wild type NJ7. The heading date of the F_2 population were recorded individually. 30 extremely early and 30 extremely late heading plants from about 200 F_2 population of each cross were selected to construct the early and late bulks. Genomic DNA of the bulks were extracted and whole-genome sequencing was performed on the two pools, generating approximately 15 Gb of total reads length with 30× coverage of genome. Gene mapping was performed based on a modified MutMap method (Abe et al. 2012). The obtained reads were aligned and annotated against the reference rice genome (Rice Genome Annotation Project: uga.edu). Subsequently, the SNP index was analyzed using previously established methods (Abe et al. 2012).

3. Reverse transcription-quantitative PCR (RT-qPCR)

The total RNA was reverse transcribed into cDNA. RT-qPCR analysis was performed using an SYBR Premix Ex Taq TM kit (TaKaRa) and an ABI prism 7500 Real-Time PCR System. RT-qPCR was performed with three technical and two biological repeats in each group. Primers were listed in Supplementary Table 3. Rice *ubiquitin* (*UBQ*) gene was applied as the internal control.

4. Subcellular localization

The full-length coding regions of *ELD4* and *OsPRR95* were ligated into the pAN580 vector to generate C-terminal GFP fusions. D53 was fused to mCherry to serve as a nuclear marker. The ELD4-GFP or OsPRR95-GFP and D53-mCherry were transiently co-expressed in rice leaf protoplasts. The method for rice leaf protoplast transformation was described previously (Zhang et al. 2019). Fluorescence signals were detected using a ZEISS LSM880 confocal microscope. Random fields were selected to photo for subcellular localization data. Primers were listed in Supplementary Table 3.

5. Yeast one-hybrid assay (Y1H) and Yeast two-hybrid assay (Y2H)

For yeast one-hybrid assay, the full-length coding regions of *ELD4* was ligated into the pB42AD vector, and a 1-kb promotor of *OsMADS51* was cloned into the pLacZi vector. Constructs and empty vectors were co-transformed into yeast strain EGY48. The transformed combinations were spread on SD/-Trp-Ura dropout medium and incubated at 30℃ for 72 hours. Grown

colonies were then transferred to color indicator medium containing X-gal, and color changes were observed.

For yeast two-hybrid assay, full-length coding regions of *ELD4* and *OsPRR95* were cloned into pGADT7 and pGBKT7 vectors. Construction and empty vectors were co-transformed into yeast strain AH109 using the Yeast marker Yeast Transformation System (Clontech). The transformed combinations were spread on SD/-Trp/-Leu and SD/–Ade/–His/–Leu/–Trp dropout mediums and incubated at 30℃ for 72 hours.

6. Bimolecular fluorescence complementation (BiFC) assay

The full-length coding regions of *ELD4*, *OsPRR95* and *OsPRMT6b* were fused with cYFP and nYFP of P2YC vector, respectively. ELD4-cYFP, OsPRR95-cYFP, OsPRR95-nYFP, OsPRMT6b-nYFP, OsPRMT6b-cYFP, empty cYFP and empty nYFP plasmids were co-transfected with the p19 silencing suppressor and a mCherry nuclear marker plasmid into *Nicotiana benthamiana* leaves using Agrobacterium tumefaciens strain GV3101. Tissues were analyzed 72 hours post-infiltration. Combinations co-transfected with empty vectors were used as negative controls. Fluorescence signals were detected using a ZEISS LSM880 confocal microscope. Random fields were selected to photo for BiFC assay.

7. *In vitro* pull down assay

ELD4-GST and OsPRR95-MBP plasmids were transformed into BL21 (DE3). Pre-cultured bacteria were transferred into 500 ml LB medium and grown at 37° C. Protein expression was induced by adding 0.5 mM isopropyl β-D-1-thiogalactopyranoside (IPTG), and cultures were incubated for 12-16 h at 16° C. Bacteria were harvested by centrifugation at 5,000 xg for 5 min and disrupted by intermittent sonication. For pull-down assay, ELD4-GST and OsPRR95-MBP fusion proteins were co-incubated with MBP resin at 4℃ for 1 hour in PBS buffer (1× PBS, 1× protease inhibitor cocktail tablets (PI, supplied from Roche) and 1 mM dithiothreitol (DTT)). MBP alone or ELD4-GST alone was co-incubated with MBP resin under the same conditions as controls. The beads were collected and washed 3-5 times with PBS buffer and examined by 10% SDS-PAGE. Western blot was conducted with GST and MBP antibodies.

8. Luciferase complementation imaging (LCI) assay

The full-length coding regions of *ELD4*, *OsPRR95* and *SHMT4* were amplified and cloned into the pCAMBIA1300-nLUC and pCAMBIA1300-cLUC vectors, respectively. Constructs were co-transformed into *Nicotiana benthamiana* leaves via Agrobacterium tumefaciens (strain GV3101)-mediated transformation. Transfected leaves were sprayed with 1 mM D-luciferin (Promega, E1602) dissolved in 0.01% (v/v) Triton X-100, and luminescence images were captured using an in vivo imaging system (Berthold, NightSHADE LB985).

9. ChIP sequencing and chromatin immunoprecipitation (ChIP)-qPCR

Chromatin immunoprecipitation (ChIP) assays were performed as previously described (Duan et al. 2019). Briefly, 5 g of leaves from ELD4-GFP overexpression lines were cross-linked in 30 ml of 1% (v/v) formaldehyde under vacuum. Chromatin was isolated from the cross-linked tissue and sheared by sonication to generate DNA fragments ranging from 200 to 500 bp. The solubilized chromatin was immunoprecipitated overnight at 4° C using anti-GFP antibody (Roche, 11814460001) conjugated to Protein A magnetic beads (Merck Millipore, 16-661). The final enriched DNA was used for sequencing or qPCR analysis. Fold enrichment was calculated as the ratio of the amount of target DNA in the immunoprecipitated (IP) sample relative to the input DNA sample.

10. Electrophoretic mobility shift assay (EMSA)

The full-length coding regions of *ELD4* and *OsPRR95* were introduced into pGEX4T-1 and pMAL-c2x vectors. The constructions and empty GST and MBP were expressed in BL21 (DE3) to induce protein expression. The proteins were purified using BeaverBeads GSH (TNLXLR0101) and amylose resin (BioLabs, E8021S) and eluted with 1×glutathione and 10 mM maltose. EMSA used the LightShift Chemiluminescent EMSA Kit (Pierce Biotechnology) to perform (Thermo, 20148). The sequences of probes are listed in Supplementary Table 3.

11. LUC activity determination

1-kb promoter and intron regions of *OsMADS51* were cloned into the pGreen0800-LUC vector (Chen et al., 2008) to create *pOsMADS51*:LUC and *iOsMADS51*:LUC construct. The full-length encode regions of *ELD4* and *OsPRR95* were transformed into pCAMBIA1390 vector to generate *ELD4-flag* and *OsPRR95-flag* constructs. *pOsMADS51*:LUC or *iOsMADS51*:LUC was co-transfected with *ELD4-flag* or *OsPRR95-flag into Nicotiana benthamiana* leaves via

Agrobacterium-mediated transformation. The Renilla reniformis (REN) driven by CaMV35S promotor was used as the control and the LUC/REN was represented the relative LUC activity. Dual-luciferase Assay Kit (Promega, E1910) was used for measuring activity.

12. The information of antibodies

For all used commercial antibodies (Dilute 5000-fold for use): Anti-GFP (Roche, Code No: 1181446000); Antibody-lgG (H + L chain) Mouse pAb-HRP (MBL, Code No: 330), which is a secondary antibody and universal for all mouse applications that require secondary antibodies; Antibody-GST (pAb-HRP-Direct Rabbit, MBL, Code No: PM013-7); Anti-MBP antibody (BioLabs, Code No: E8032S).

Statistical analysis

The statistical results are presented as means ± SD, with n denoting the number of biological replicates. Two-tailed student's *t*-tests were performed for two groups comparisons. The statistical methods used for each experiment are both detailed in the figure legends. Three separate plants per tissue sample were combined to form three biological replicates in RT-qPCR analysis. Each experiment was performed a minimum of three times to ensure consistency. Detailed statistical analysis data are provided as Supplementary Data Set 2.

Accession numbers

The sequences of the genes related to this study are available on the Rice Genome Annotation Project website at https://rice.uga.edu/. The accession number mentioned in this article: *ELD4 (LOC_Os09g35880)*, *OsPRR95 (LOC_Os09g36220)*, *OsMADS51 (LOC_Os01g69850)*, *SHMT4 (LOC_Os01g65410)*, *OsPRMT6b (LOC_Os04g58060), Ghd2 (LOC_Os02g49880)*.

Author contributions

J. M. W. supervised the study. S. S. Z., S. R. Z. and X. J. conceived the study and designed the experiments. W. L., X. Y. Z., F. Q. W., Y. P. W., Y. M. L., J. W., L. Z. M., X. L., M. X. W., L. M. Z., X. D. Z. and Q. Y. Y. participated in partial biochemical experiments. Z. W. L. analyzed

data. Y. L. R., C. L. L., Q. B. L., Z. J. C., Z. C. Z., X. P. G. and X. W. participated in rice transformation. X. J., S. S. Z. and S. R. Z. wrote and revised the article.

Funding

This work was supported by the National Key Research and Development Program of China (2022YFD1201500), Biological Breeding-National Science and Technology Major Project (2023ZD04072), Innovation Program of Chinese Academy of Agricultural Sciences and the earmarked fund for CARS-01-05.

Data availability

All data supporting the finding of this work are available in the article and its Supplementary Information files. Plant materials generated in this study are available from the corresponding author upon request. RT-PCR data applied ABI prism 7500 Real-Time PCR System. Subcellular localization and BiFC assay applied ZEISS LSM880 confocal microscope. LCI assay applied imaging apparatus (Berthold, LB985). ImageJ was used for the quantitative analysis of all western blot. The software R 4.3.1 was used to create box plots of heading date. DNAMAN 9.0 software is used for protein sequence alignment. The gene structures of *ELD4*, *OsPRR95* and *OsMADS51* are from NCBI (https://www.ncbi.nlm.nih.gov/); Homologs were obtained from NCBI BLAST (https://blast.ncbi.nlm.nih.gov/Blast.cg). The target sites of primer design obtained from the CRISPR-P 2.0 website (http://cbi.hzau.edu.cn/cgi-bin/CRISPR). Nipponbare reference genome is available at Gramene website (http://www.gramene.org). The raw data of ChIP-seq generated in this study have been deposited in the NCBI database under the BioProject ID: PRJNA1291839.

References

Abe A, Kosugi S, Yoshida K, Natsume S, Takagi H, Kanzaki H, Matsumura H, Yoshida K, Mitsuoka C, Tamiru M et al., Genome sequencing reveals agronomically important loci in rice. Nat Biotechnol. 2012: 30 (2): 174-8. https://doi.org/10.1038/nbt.2095.

Andrade L, Lu YL, Cordeiro A, Costa JMF, Wigge PA, Saibo NLM, Jaeger K. The evening complex integrates photoperiod signals to control flowering in rice. Proc Natl Acad Sci U S A. 2022: 119 (26): e2122582119. https://doi.org/10.1073/pnas.2122582119.

Beales J, Turner A, Griffiths S, Snape JW, Laurie DA. A pseudo-response regulator is misexpressed in the photoperiod insensitive Ppd-D1a mutant of wheat (Triticum aestivum L.). Theor Appl Genet. 2007: 115 (5) 721–733. http: //doi: 10.1007/s00122-007-0603-4.

Cai MH, Zhu SS, Wu MM, Zheng XM, Wang JC, Zhou L, Zheng TH, Cui S, Zhou SR, Li CN et al. DHD4, A CONSTANS-like Family Transcription Factor, Delays Heading Date through Affecting the Formation of FAC Complex in Rice. Mol Plant. 2020: 14 (2): 330-343. https://doi.org/10.1016/j.molp.2020.11.013.

Chai JT, Zhu SS, Li CN, Wang CM, Cai MH, Zheng XM, Zhou L, Zhang H, Sheng PK, Wu MM et al. OsRE1 interacts with OsRIP1 to regulate rice heading date by finely modulating Ehd1 expression. Plant Biotechnol J. 2021: 19 (2): 300-310. https://doi.org/10.1111/pbi.13462.

Chen CQ, Tian XY, Li J, Bai S, Zhang ZY, Li Y, Cao HR, Chen ZC. Two central circadian oscillators OsPRR59 and OsPRR95 modulate magnesium homeostasis and carbon fixation in rice. Mol Plant. 2022: 15 (10): 1602-1614. http:// doi: 10.1016/j.molp.2022.09.008.

Chen HM, Zou Y, Shang YL, Lin HQ, Wang YJ, Cai R, Tang XY, Zhou JM. Firefly luciferase complementation imaging assay for protein–protein interactions in plants. Plant Physiol. 2008: 146(2): 323–324. https://doi.org/10.1104/pp.107.111740.

Chen JY, Zhang HW, Zhang HL, Ying JZ, Ma LY, Zhuang JY. Natural variation at qHd1 affects heading date acceleration at high temperatures with pleiotropism for yield traits in rice. BMC Plant Biol. 2018: 18 (1): 112. http:// doi: 10.1186/s12870-018-1330-5.

Datta S, Hettiarachchi C, Johansson H, Holm M. SALT TOLERANCE HOMOLOG2, a B-Box protein in Arabidopsis that activates transcription and positively regulates light-mediated development. Plant Cell. 2007: 19 (10): 3242-3255. http://doi: 10.1105/tpc.107.054791.

Datta S, Hettiarachchi ETTIARACHCHI GHCM, Deng XW, Holm M. Arabidopsis CONSTANS-LIKE3 is a positive regulator of red light signaling and root growth. Plant Cell. 2006: 18 (1): 70-84. http://doi: 10.1105/tpc.105.038182.

Datta S, Johansson H, Hettiarachchi C, Irigoyen ML, Desai M, Rubio V, Holm M. LZF1/SALT TOLERANCE HOMOLOG3, an Arabidopsis B-Box Protein Involved in Light-Dependent Development and Gene Expression, Undergoes COP1-Mediated Ubiquitination. Plant Cell. 2008: 20 (9): 2324-2338. http://doi: 10.1105/tpc.108.061747.

Doi K, Izawa T, Fuse T, Yamanouchi U, Kubo T, Shimatani Z, Yano M, Yoshimura A. Ehd1, a B-type response regulator in rice, confers short-day promotion of flowering and controls FT-like gene expression independently of *Hd1*. Genes Dev. 2004: 18 (8):926–936. http:// doi: 10.1101/gad.1189604. Epub 2004 Apr 12.

Duan EC, Wang YH, Li XH, Lin QB, Zhang T, Wang YP, Zhou CL, Zhang H, Jiang L, Wang JL et al. OsSHI1 regulates plant architecture through modulating the transcriptional activity of IPA1 in rice. Plant Cell. 2019: 31(5): 1026–1042. https://doi.org/10.1105/tpc.19.00023.

Fan XY, Sun Y, Cao DM, Bai MY, Luo XM, Yang HJ, Wei CQ, Zhu SW, Sun Y, Chong K et al. BZS1, a B-box Protein, Promotes Photomorphogenesis Downstream of Both Brassinosteroid and Light Signaling Pathways. Mol Plant. 2012: 5 (3): 591-600. http://doi: 10.1093/mp/sss041.

Fornara F, Panigrahi KCS, Gissot L, Sauerbrunn N, Rühl M, Jarillo JA, Coupland G. Arabidopsis DOF transcription factors act redundantly to reduce CONSTANS expression and are essential for a photoperiodic flowering response. Dev. Cell. 2009: 17 (1): 75–86. https://doi.org/10.1016/j.devcel.2009.06.015.

Fu MX, Liu SS, Che YQ, Cui DD, Deng ZY, Li Y, Zou XY, Kong XC, Chen GL, Zhang M et al. Genome-editing of a circadian clock gene TaPRR95 facilitates wheat peduncle growth and

heading date. J Genet Genomics. 2024: 51(10): 1101-1110. http://doi: 10.1016/j.jgg.2024.05.011.

Gangappa SN, Botto JF. The BBX family of plant transcription factors. Trends Plant Sci. 2014: 19 (7): 460-470. http://doi: 10.1016/j.tplants.2014.01.010.

Gangappa SN, Crocco CD, Johansson H, Datta S, Hettiarachchi C, Holm M, Botto JF. The Arabidopsis B-BOX Protein BBX25 Interacts with HY5, Negatively Regulating BBX22 Expression to Suppress Seedling Photomorphogenesis. Plant Cell. 2013: 25 (4): 1243-1257. http://doi: 10.1105/tpc.113.109751.

Gao H, Jin MN, Zheng XM, Chen J, Yuan DY, Xin YY, Wang MQ, Huang DY, Zhang Z, Zhou KN et al. Days to heading 7, a major quantitative locus determining photoperiod sensitivity and regional adaptation in rice. Proc Natl Acad Sci U S A. 2014: 111 (46): 16337-16342. http:// doi: 10.1073/pnas.1418204111.

Hayama R, Yokoi S, Tamaki S, Yano M, Shimamoto K. Adaptation of photoperiodic control pathways produces short-day flowering in rice. Nature. 2003: 422: 719–722. https://doi.org/10.1038/nature01549.

Holm M, Hardtke CS, Gaudet R, Deng XW. Identification of a structural motif that confers specific interaction with the WD40 repeat domain of Arabidopsis COP1. Embo J. 2001: 20 (1-2): 118-127. http://doi: 10.1093/emboj/20.1.118.

Holtan HE, Bandong S, Marion CM, Adam L, Tiwari S, Shen Y, Maloof JN, Maszle DR, Ohto MA, Preuss S et al. BBX32, an Arabidopsis B-Box Protein, Functions in Light Signaling by Suppressing HY5-Regulated Gene Expression and Interacting with STH2/BBX21. Plant Physiol. 2011: 156 (4): 2109-2123. http://doi: 10.1104/pp.111.177139.

Hu Y, Zhou X, Zhang B, Li SL, Fan XW, Zhao H, Zhang J, Liu HY, He Q, Li QP et al. OsPRR37 alternatively promotes heading date through suppressing the expression of Ghd7 in the Japonica variety Zhonghua 11 under natural long-day conditions. Rice. 2021: 14(1): 20. http://doi: 10.1186/s12284-021-00464-1.

Huang JY, Zhao XB, Weng XY, Wang L, Xie WB. The rice b-box zinc finger gene family: genomic identification, characterization, expression profiling and diurnal analysis. PLoS One. 2012: 7 (10): e48242. http://doi: 10.1371/journal.pone.0048242.

Jin X, Lin QB, Zhang XY, Zhang S, Ma Weiwei, Sheng Peike, Zhang LM, Wu MX, Zhu XD, Li ZW et al. OsPRMT6b balances plant growth and high temperature stress by feedback inhibition of abscisic acid signaling. Nat Commun. 2025: 16 (1): 5173. http://doi: www.nature.com/articles/s41467-025-60350-y.

Khanna R, Kronmiller B, Maszle DR, Coupland G, Holm M, Mizuno T, Wu SH. The Arabidopsis b-box zinc finger family, Plant Cell. 2009: 21 (11): 3416-3420. http://doi: 10.1105/tpc.109.069088.

Khanna R, Shen Y, Tolendo-Ortiz G, Kikis E A, Johannesson H, Hwang YS, Quail PH. Functional profiling reveals that only a small number of phytochrome-regulated early-response genes in Arabidopsis are necessary for optimal deterioration. Plant Cell. 2006: 18 (9): 2157-2171. http://doi: 10.1105/tpc.106.042200.

Klug A, W. R. Schwabe J. Zinc Fingers. Faseb J. 1995: 9(8): 597-604. https://doi.org/10.1096/fasebj.9.8.7768350.

Kojima S, Takahashi YJ, Kobayashi Y, Monna L, Sasaki T, ArakiT, Yano M. Hd3a, a rice ortholog of the Arabidopsis FT gene, promotes transition to flowering downstream of Hd1 under short-day conditions. Plant Cell Physiol. 2002: 43 (10): 1096–1105. http://doi: 10.1093/pcp/pcf156.

Koo BH, Yoo SC, Park JW, Kwon CT, Lee BD, An G, Zhang ZY, Li JJ, Li ZC, Paek NC. Natural variation in OsPRR37 regulates heading date and contributes to rice cultivation at a wide range of latitudes, Mol Plant. 2013: 6 (6): 1877–1888. http:// doi: 10.1093/mp/sst088.

Kumagai T, Ito S, Nakamichi N, Niwa Y, Murakami M, Yamashino T, Mizuno T. The common function of a novel subfamily of B-box zinc finger proteins with reference to circadian-associated events in Arabidopsis thaliana. Biosci Biotechnol Biochem. 2008: 72 (6): 1539-1549. http://doi: 10.1271/bbb.80041.

Kim SL, Lee S, Kim HJ, Nam HG, An G. OsMADS51 is a short-day flowering promoter that functions upstream of Ehd1, OsMADS14, and Hd3a, Plant Physiol. 2007: 145: 1484‑1494. http://doi: 10.1104/pp.107.103291.

Li F, Sun JJ, Wang DH, Bai SN, Clarke AK, Holm M. The B-box family gene STO (BBX24) in Arabidopsis thaliana regulates flowering time in different pathways. PloS One. 2014: 9(2): e87544. http://doi: 10.1371/journal.pone.0087544.

Li Y, Yu YJ, Liu MM, Song Y, Li HM, Sun JQ, Wang Q, Xie QG, Wang L, X, XD. BBX19 fine-tunes the circadian rhythm by interacting with PSEUDO-RESPONSE REGULATOR proteins to facilitate their repressive effect on morning-phased clock genes. Plant Cell. 2021: 33 (8): 2602–2617. http:// doi: 10.1093/plcell/koab133.

Liu C, Qu XF, Zhou YH, Song GY, Abiri N, Xiao YH, Liang F, Jiang DM, Hu ZL, Yang DC. OsPRR37 confers an expanded regulation of the diurnal rhythms of the transcriptome and photoperiodic flowering pathways in rice. Plant Cell Environ. 2018: 41 (3): 630–645. http:// doi: 10.1111/pce.13135.

Matsushika A, Makino S, Kojima M, Mizuno T. Circadian waves of expression of the APRR1/TOC1 family of pseudo-response regulators in Arabidopsis thaliana: insight into the plant circadian clock. Plant Cell Physiol. 2000: 41(9): 1002-1012. http:// doi: 10.1093/pcp/pcd043.

Murakami M, Tago Y, Yamashino T, Mizuno T. Characterization of the rice circadian clock-associated pseudo-response regulators in Arabidopsis thaliana, Biosci Biotechnol Biochem. 2007: 71 (4): 1107–1110. http:// doi: 10.1271/bbb.70048.

Murphy RL, Klein RR, Morishige DT, Brady JA, Rooney WL, Miller FR, Dugas DV, Klein PE, Mullet JE. Coincident light and clock regulation of pseudo response regulator protein 37 (PRR37) controls photoperiodic flowering in sorghum. Proc Natl Acad Sci U S A. 2011: 108 (39): 16469–16474. http:// doi: 10.1073/pnas.1106212108.

Nagaoka S, Takano T. Salt tolerance-related protein STO binds to a Myb transcription factor homologue and confers salt tolerance in Arabidopsis. J Exp Bot. 2003: 54 (391): 2231-2237. http://doi: 10.1093/jxb/erg241.

Nakamichi N, Kiba YT, Henriques R, Mizuno T, Chua NH, Sakakibara. PSEUDO-RESPONSE REGULATORS 9, 7, and 5 are transcriptional repressors in the Arabidopsis circadian clock, Plant Cell. 2010: 22 (3): 594–605. http:// doi: 10.1105/tpc.109.072892.

Nakamichi N, Kita M, Ito S, Yamashino T, Mizuno T. PSEUDO-RESPONSE REGULATORS, PRR9, PRR7 and PRR5, together play essential roles close to the circadian clock of Arabidopsis thaliana, Plant Cell Physiol. 2005: 46 (5): 686–698. http:// doi: 10.1093/pcp/pci086.

Song YH, Ito S, Imaizumi T. Flowering time regulation: photoperiod- and temperature-sensing in leaves. Trends Plant Sci. 2013: 18 (10): 575–583. https://doi.org/10.1016/j.tplants.2013.05.003.

Sun KL, Huang MH, Zong WB, Xiao DD, Lei C, Luo YQ, Song YG, Li ST, Hao Y, Luo WN et al. Hd1, Ghd7, and DTH8 synergistically determine rice heading date and yield-related agronomic traits. J Genet Genomics. 2022: 49 (5): 437-447. https://doi.org/10.1016/j.jgg.2022.02.018.

Tamaki S, Matsuo S, Wong HL, Yokoi S, Shimamoto K. Hd3a protein is a mobile flowering signal in rice. Science. 2007: 316 (5827): 1033–1036. http:// doi: 10.1126/science.1141753. Epub 2007 Apr 19.

Turner A, Beales J, Faure S, Dunford RP, Laurie DA. The pseudo-response regulator Ppd-H1 provides adaptation to photoperiod in barley. Science. 2005: 310 (5750): 1031–1034. http:// doi: 10.1126/science.1117619.

Wang B, Li JY. Understanding the molecular bases of agronomic trait improvement in rice. Plant Cell. 2019: 31 (7): 1416-1417. https://doi.org/10.1105/tpc.19.00343.

Wang CQ, Guthrie C, Sarmast MK, Dehesh K. BBX19 interacts with CONSTANS to repress FLOWERING LOCUS T transcription, defining a flowering time checkpoint in Arabidopsis. Plant Cell. 2014: 26 (9): 3589-3602. http:// doi: 10.1105/tpc.114.130252.

Wang LW, Sun S, Wu TT, Liu LP, Sun XG, Cai YP, Li JC, Jia HC, Yuan S, Chen L et al. Natural variation and CRISPR/Cas9-mediated mutation in GmPRR37 affect photoperiodic

flowering and contribute to regional adaptation of soybean, Plant Biotechnol J. 2020: 18 (9): 1869–1881. http:// doi: 10.1111/pbi.13346.

Wang QM, Tu XJ, Zhang JH, Chen XB, Rao LQ. Heat stress-induced BBX18 negatively regulates the thermotolerance in Arabidopsis. Mol Biol Rep. 2013: 40 (3): 2679-2688. http://doi: 10.1007/s11033-012-2354-9.

Wang YP, Wu FQ, Zhou SR, Chen WW, Li CN, Duan EC, Wang JC, Cheng ZJ, Zhang X, Lin Q et al. Clock component OsPRR59 delays heading date by repressing transcription of Ehd3 in rice. Crop J. 2022: 10 (6): 1570-1579. https://doi.org/10.1016/j.cj.2022.04.007.

Xu DQ, Jiang Y, Li JG, Lin F, Holm M, Deng XW. BBX21, an Arabidopsis B-box protein, directly activates HY5 and is targeted by COP1 for 26S proteasome-mediated degradation. Proc Natl Acad Sci U S A. 2016: 113 (27): 7655‑7660. http:// doi: 10.1073/pnas.1607687113.

Xu ZT, Li E, Xue G, Zhang C, Yang YH, Ding Y. OsHUB2 inhibits function of OsTrx1 in heading date in rice. Plant J. 2022: 110 (6):1670-1680. http:// doi: 10.1111/tpj.15763.

Xue WY, Xing YZ, Weng XY, Zhao Y, Tang WJ, Wang L, Zhou HJ, Yu AB, Xu CG, Li XH et al. Natural variation in Ghd7 is an important regulator of heading date and yield potential in rice. Nat Genet. 2008: 40 (6): 761-767. http:// doi: 10.1038/ng.143.

Yan WH, Wang P, Chen HX, Zhou HJ, Li QP, Wang CR, Ding ZH, Zhang YS, Yu SB, Xing YZ et al. A major QTL, Ghd8, plays pleiotropic roles in regulating grain productivity, plant height, and heading date in rice. Mol Plant. 2011: 4 (2): 319-330. http:// doi: 10.1093/mp/ssq070.

Yang ML, Han X, Yang JJ, Jiang YJ, Hu YR. The Arabidopsis circadian clock protein PRR5 interacts with and stimulates ABI5 to modulate abscisic acid signaling during seed germination. Plant Cell. 2021: 33 (9): 3022–3041. http:// doi: 10.1093/plcell/koab168.

Yano M, Katayose Y, Ashikari M, Yamanouchi U, Monna L, Fuse T, Baba T, Yamamoto K, Umehara Y, Nagamura Y et al. Hd1, a major photoperiod sensitivity quantitative trait locus in rice, is closely related to the arabidopsis flowering time gene CONSTANS. Plant Cell. 2000: 12 (12): 2473–2483. http:// doi: 10.1105/tpc.12.12.2473.

Yan MY, Pan T, Zhu Y, Jiang XK, Yu MZ, Wang RQ, Zhang F, Luo S, Bao XH, Chen Y et al. FLOURY ENDOSPERM20 encoding SHMT4 is required for rice endosperm development. Plant Biotechnol J. 2022: 20 (8):1438-1440. http:// doi: 10.1111/pbi.13858.

Yu YJ, Su C, He YQ, Wang L. B-Box proteins BBX28 and BBX29 interplay with PSEUDO-RESPONSE REGULATORS to fine-tune circadian clock in Arabidopsis. Plant Cell Environ. 2023: 46 (9): 2810-2826. http:// doi: 10.1111/pce.14648.

Zhang H, Zhu SS, Liu TZ, Wang CM, Cheng ZJ, Zhang X, Chen LP, Sheng PK, Cai MH, Li CN et al. DELAYED HEADING DATE1 interacts with OsHAP5C/D, delays flowering time and enhances yield in rice. Plant Biotechnol J. 2019: 17 (2): 531-539. http:// doi: 10.1111/pbi.12996.

Zhang Y, Su JB, Duan S, Ao Y, Dai JR, Liu J, Wang P, Li YG, Liu B, Feng DR et al. A highly efficient rice green tissue protoplast system for transient gene expression and studying light/chloroplast-related processes. Plant Methods. 2011: 7: 30. https://doi.org/10.1186/1746-4811-7-30.

Zhao L, Hu HF, Chen JY, Wang CR, Chen YB, Li H, Huang DQ, Wang ZD, Zhou DG, Gong R et al. A 9.5-kb deletion in the 1st intron of OsMADS51 enhances temperature sensitivity in rice. Crop J. 2024: 12 (4):1031-1040 (2024). https://doi.org/10.1016/j.cj.2024.05.010.

Zhou F, Lin QB, Zhu LH, Ren YL, Zhou KN, Shabek N, Wu FQ, Mao HB, Dong W, Gan L et al. D14-SCF(D3)-dependent degradation of D53 regulates strigolactone signalling. Nature. 2013: 504(7480): 406-410. http:// doi: 10.1038/nature16537.

Figure 1. The phenotypes of *eld4-1* obtained by the modified MutMap and *ELD4* knockout, overexpression and RNAi lines

(A) The phenotypes of WT and *eld4-1* mutant. Bars, 20 cm. (B) The heading date of WT and *eld4-1* mutant. Data are means ± SD (n = 17 seedlings). (C) Bulk segregant analysis of genes responsible for the heading date phenotypes of *eld4-1*. The significance of each single nucleotide polymorphisms (SNPs) on 12 chromosomes between early and late bulks are indicated. (D) Schematic diagram of structure of the *LOC_Os09g35880* gene. Black boxes, grey boxes and

lines indicate exons, UTRs and introns, respectively. The purple and blue boxes represent the first and second B-Box domains, respectively. The red words represent the sites of nucleotide mutation and amino acid substitutions in *eld4-1* mutant. (E) The flowering phenotypes of WT and *eld4* mutants under NLD conditions. *eld4-4* and *eld4-5* represented two independent CRISPR/Cas9 knockout lines of *ELD4*. Bar, 15 cm. The white arrow indicated panicles. (F) The flowering phenotypes of WT and *ELD4* overexpression lines under NLD conditions. *OE-ELD4-1* and *OE-ELD4-2* represented two independent lines of *ELD4* overexpression plants. Bar, 15cm. The white arrow indicated panicles. (G) The expression level of *ELD4* overexpression lines. Data, means ± SD (n = three biological replicates). (H) The heading date of WT, *eld4* mutants and *ELD4* overexpression lines under NLD conditions. Data are means ± SD (n = 10 seedlings). (I) The gene structure diagram of *ELD4* and the target sequence of *eld4* mutant by CRISPR/Cas9 system. The green boxes and lines represented the exons and introns, respectively. The sequencing chromatograms of *eld4* mutants were attached. (J) The phenotype of Aso, *eld4-6* and *eld4-7* transgenic lines. Bar, 15 cm. The white arrow indicated panicles. (K) The heading date of Aso, *eld4-6* and *eld4-7* transgenic lines. Data are means ± SD (n = 14 seedlings). (L) The phenotype of WT, *ELD4RNAi-2* and *ELD4RNAi-4* transgenic lines. Bar, 15 cm. The white arrow indicated panicles. (M) The heading date of WT, *ELD4RNAi-2* and *ELD4RNAi-4* transgenic lines. Data are means ± SD (n = 14 seedlings).

All above *P* values were calculated by two-tailed *t*-test.

Figure 2. The expression pattern and subcellular localization of ELD4

(A) The relative expression levels of *ELD4* in different rice tissues. Data are means ± SD (n = three biological replicates). (B and C) The rhythmic expression of *ELD4* under LD (B) and SD (C). ZT, Zeitgeber Time. Data were means ± SD (n = three biological replicates). The rice *UBIQUITIN* (*UBQ*) gene was used as the internal control. (D) The subcellular localization of ELD4-GFP in rice protoplasts. Empty GFP was used as the internal control (n = three independent experiments). Bar, 10 μm. The mCherry fused with D53 protein was used as the nuclear marker. Merged, the fusion channel of GFP channel, mCherry channel and Bright Field channel.

Figure 3. ELD4 interacted with OsPRR95

(A) Yeast two-hybrid (Y2H) assay showing ELD4 interacted with OsPRR95. Empty AD and BD were used as the control (n = three independent experiments). (B) Bimolecular fluorescence complementation (BiFC) assays showing the interaction between ELD4 and OsPRR95 in the tobacco leaves (n = three independent experiments). The mCherry fused with D53 protein was used as the nuclear marker. The coding regions of ELD4 and OsPRR95 were fused with cYFP and nYFP, respectively. OsPRMT6b (Jin et al. 2025) was used for the control. Merged, the fusion channel of YFP channel, mCherry channel and Bright Field channel. YFP, green signal; mCherry, purple signal. Bar, 10 μm. (C) *In vitro* pull-down assay showing the interaction between ELD4 and OsPRR95 (n = three independent experiments). The fusion proteins were pulled down by MBP resin. Antibodies against MBP and GST were used for western blot analysis. MBP was used as the control. (D) Luciferase complementation imaging (LCI) assay proved that ELD4 interacted with OsPRR95 in tobacco leaves (n = three independent experiments). SHMT4 (Yan et al. 2022) was used as the control.

Figure 4 ELD4 and OsPRR95 co-regulated the heading date in rice

(A) The phenotypes of WT and *Osprr95* mutants under NLD conditions. Bar, 15 cm. The white arrow indicated panicles. (B) The heading date of WT and *Osprr95* mutants under NLD and NSD conditions. Data are means ± SD (n = 15 seedlings). (C) The phenotypes of ZH11, *Osprr95-3* and *Osprr95-4* transgenic lines. Bar, 15 cm. The white arrow indicated panicles. (D) The gene structure diagram of *OsPRR95* and the sequence of *Osprr95* mutant by CRISPR/Cas9 system. Sequence alignment indicates the *Osprr95* mutant carries a 9-bp deletion in the 5′ UTR that encompasses the initiator ATG. The green boxes and lines represented the exons and introns, respectively. The sequencing chromatograms of *Osprr95* mutants were attached. (E) The heading date of ZH11, *Osprr95-3* and *Osprr95-4* transgenic lines. Data are means ± SD (n = 13 seedlings). (F) The phenotypes of ZH11, *OE-OsPRR95-2* and *OE-OsPRR95-3* transgenic lines. Bar, 25 cm. The white arrow indicated panicles. (G) The relative expression level of *OsPRR95* in ZH11, *OE-OsPRR95-2* and *OE-OsPRR95-3* transgenic lines. Data are means ± SD (n = three

biological replicates). (H) The heading date of ZH11, *OE-OsPRR95-2* and *OE-OsPRR95-3* transgenic lines. Data are means ± SD (n = 16 seedlings). (I) The phenotypes of WT, *Osprr95*, *eld4* and *eld4 Osprr95* mutants under NLD conditions. Bar, 15 cm. The white arrow indicated panicles. (J) The heading date of WT, *Osprr95*, *eld4* and *eld4 Osprr95* mutants under NLD and NSD conditions. Data are means ± SD (n = 13 seedlings).

All above *P* values were calculated by two-tailed *t*-test.

Figure 5 The basic properties and self-interaction of OsPRR95

(A) The expression levels of *OsPRR95* in different rice tissues. Data are means ± SD (n = three biological replicates). (B and C) The rhythmic expression pattern of *OsPRR95* under LD (B) and SD (C). ZT, Zeitgeber Time. Data were means ± SD (n = three biological replicates). The rice *ubiquitin* (*UBQ*) gene was used as the internal control. (D) The subcellular localization of OsPRR95-GFP in rice protoplasts. Empty GFP was used as the internal control (n = three independent experiments). Bar, 5 μm. (E and F) Transcription activity assay indicated that OsPRR95 is a transcriptional repressor. The empty BD was used as the control. Data are means ± SD (n = three independent experiments). *P* value was calculated by two-tailed *t*-test. (G) Yeast two-hybrid (Y2H) assay showing OsPRR95 interacted with OsPRR95. Empty AD and BD were used as the control (n = three independent experiments). (H) Luciferase complementation imaging (LCI) assay showed that OsPRR95 can interact with itself in tobacco leaves. SHMT4-cLUC and SHMT4-nLUC (Yan et al. 2018) were used as the negative control (n = three independent experiments). (I) Bimolecular fluorescence complementation (BiFC) assays showing that OsPRR95 can form a homodimer in the tobacco leaves. OsPRMT6b was used as the control. The mCherry fused with D53 protein was used as the nuclear marker (n = three independent experiments). The coding region of *OsPRR95* was fused with cYFP and nYFP, respectively. Merged, the fusion channel of YFP channel, mCherry channel and Bright Field channel. Bar, 10 μm. YFP, green signal; mCherry, purple signal.

Figure 6 ELD4 and OsPRR95 bound to the promoter and first intron of *OsMADS51*

(A) The schematic diagram of structure of *OsMADS51*. Black boxes, grey boxes and lines indicate exons, UTRs and introns, respectively. (B) ChIP-qPCR assay showing that ELD4 bound to the promotor and intron of *OsMADS51. ELD4* overexpression lines and GFP antibodies were used for ChIP assay. P1-P5 primers were exhibited in A. Data were means ± SD (n = three independent experiments). (C and D) EMSA assay showing that ELD4 and OsPRR95 bound to the G-box in the promotor and the intron of *OsMADS51.* G-Box^{-Bio} and R motif^{-Bio} are the target probe, and G-Box-Comp and R motif-Comp are the competitor probe. Plus (+) and minus (-) represented the presence and absence of the probe or protein in each combination. The arrow indicates the binding shift (n = three independent experiments). (E and F) Transcription activity assays indicating that ELD4 and OsPRR95 suppressed the activity of *OsMADS51*. The effectors and reporters were shown in (E). The relative transcription activities were calculated by LUC/REN (n = three independent experiments). (G) EMSA assays showing that ELD4 enhances the binding of OsPRR95 to the intron of *OsMADS51*. Plus (+) and minus (-) represented the presence and absence of the probe or protein in each combination. R motif^{-Bio} is the target probe. The arrow indicates the binding shift (n = three independent experiments). (H) Transcription activity assays indicating that ELD4 enhanced OsPRR95-mediated repression of the first intron of *OsMADS51*. The bar chart on the right represents the corresponding relative fluorescence intensity (n = two independent experiments). (I) The phenotypes of WT, *OE-ELD4*, *OE-OsMADS51* and *OE-ELD4 OsMADS51* transgenic lines under NLD conditions. The full-length coding region of *OsMADS51* was cloned into the pCAMBIA1390 vector. Bar, 15 cm. The white arrow indicated panicles. (J) The heading date of WT, *OE-ELD4*, *OE-OsMADS51* and *OE-ELD4 OsMADS51* transgenic lines under NLD conditions. Data are means ± SD (n = 16 seedlings).

All above *P* values were calculated by two-tailed *t*-test.

Figure 7 The haplotypes of *OsPRR95* with heading date in rice

(A) The main haplotypes of *OsPRR95* in RiceVarMap 2.0 database (https://ricevarmap.ncpgr.cn/hap_net/). The figure below shows the gene structure diagram of *OsPRR95* and the locations of SNPs (Single Nucleotide Polymorphisms). (B) Heading date

phenotypes of the four haplotypes. Student's *t*-tests was used for significance analysis (*P <0.05, **P <0.01). (C) Significance analysis of heading date phenotypes among four haplotypes. (D) Distribution of rice varieties among the four haplotypes. (E) Geographic distribution of Hap 1 and Hap 3. The x- and y-axes represent longitude and latitude, respectively.

Figure 8 The working model of ELD4-OsPRR95 in regulating heading

In WT, the OsPRR95 dimer interacts with ELD4 to co-bind to the first intron and promoter of *OsMADS51*, thereby repressing *OsMADS51* expression and delaying rice flowering. ELD4 also enhances the repressive effect of OsPRR95 on *OsMADS51*. In the *Osprr95* mutant, the lack of OsPRR95 protein alleviates the suppression of *OsMADS51*, resulting in a significant release of *OsMADS51* and a subsequent boost in florigens production, thereby accelerating rice heading. In the *eld4* mutant, the downstream loss of ELD4 entirely eliminates the repressive effects of both OsPRR95 and ELD4 on *OsMADS51*, thereby promoting a robust increase in florigen production and a pronounced acceleration of heading time.

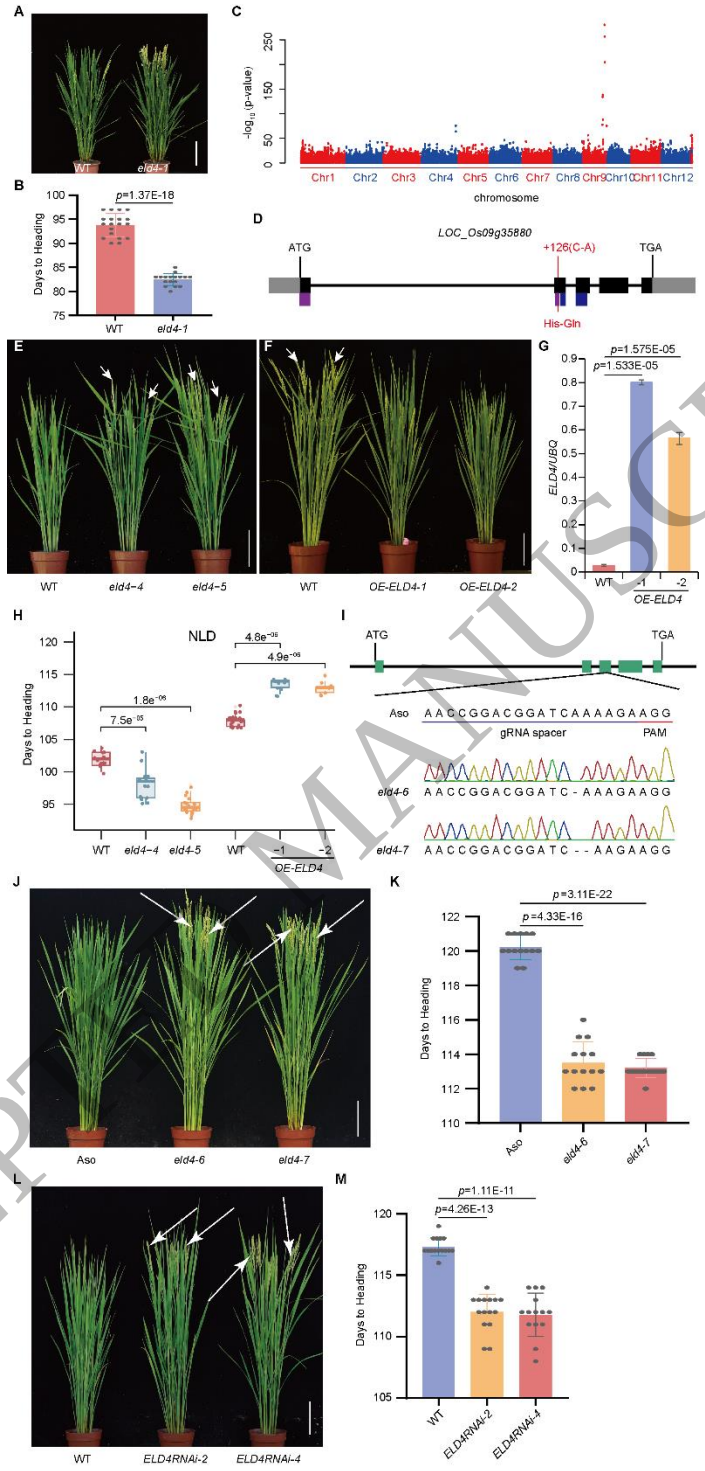

Figure 1
108x229 mm (x DPI)

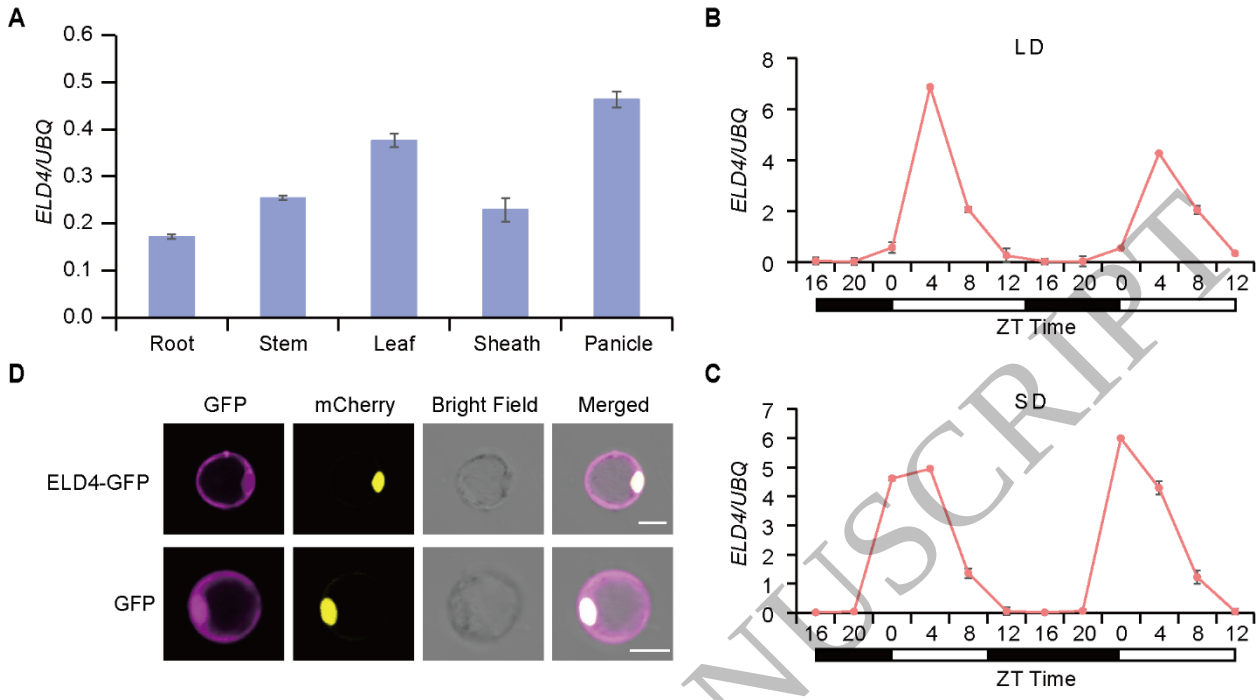

Figure 2
165x105 mm (x DPI)

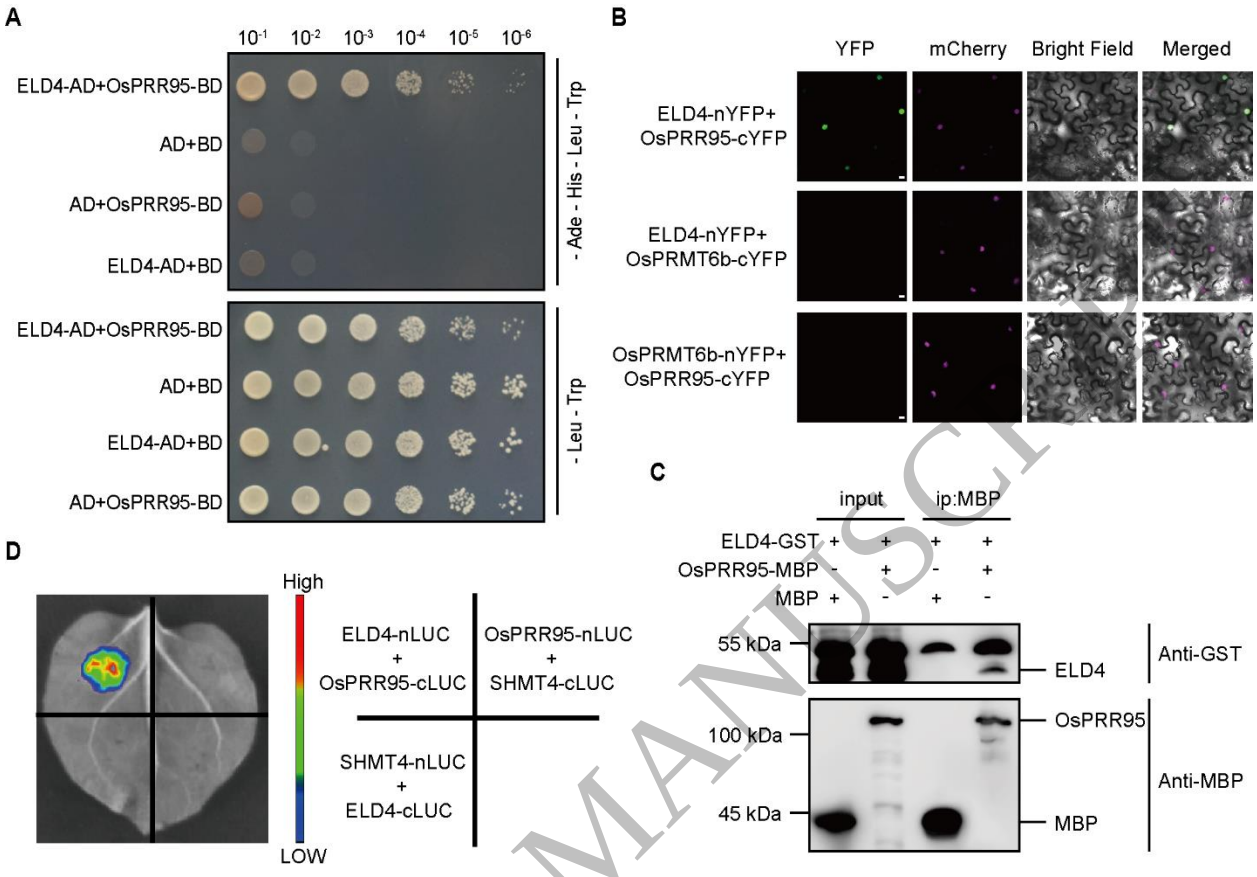

Figure 3
165x114 mm (x DPI)

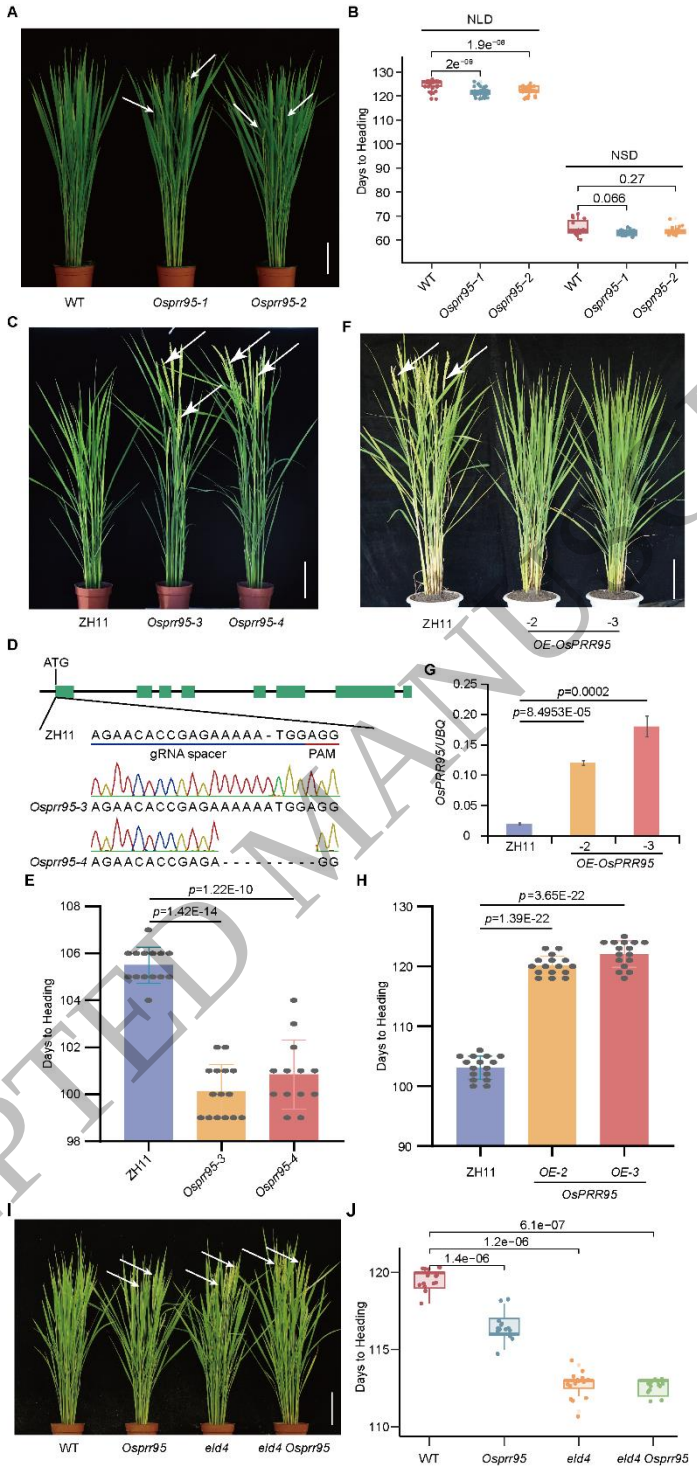

Figure 4
107x229 mm (x DPI)

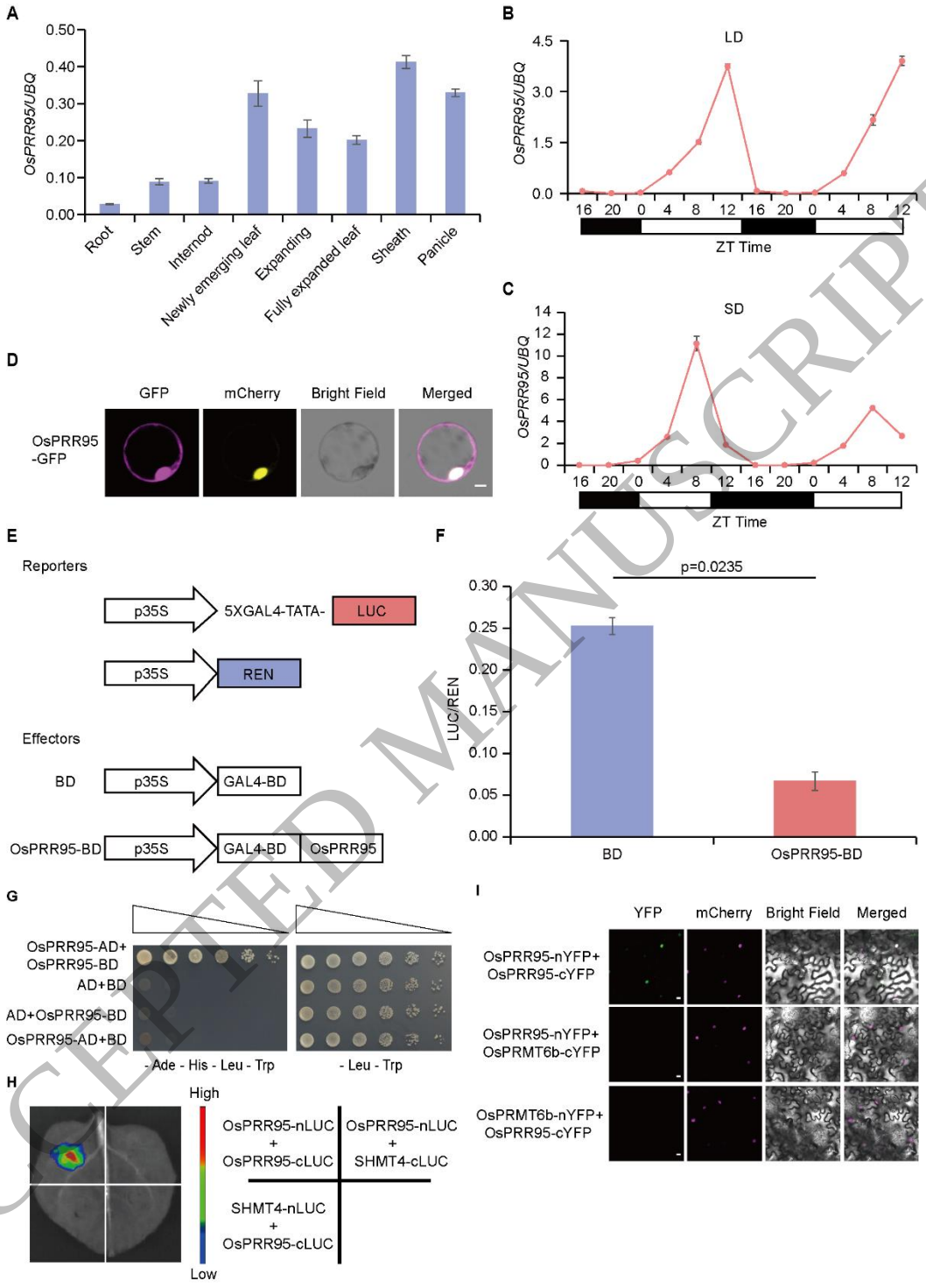

Figure 5
163x229 mm (x DPI)

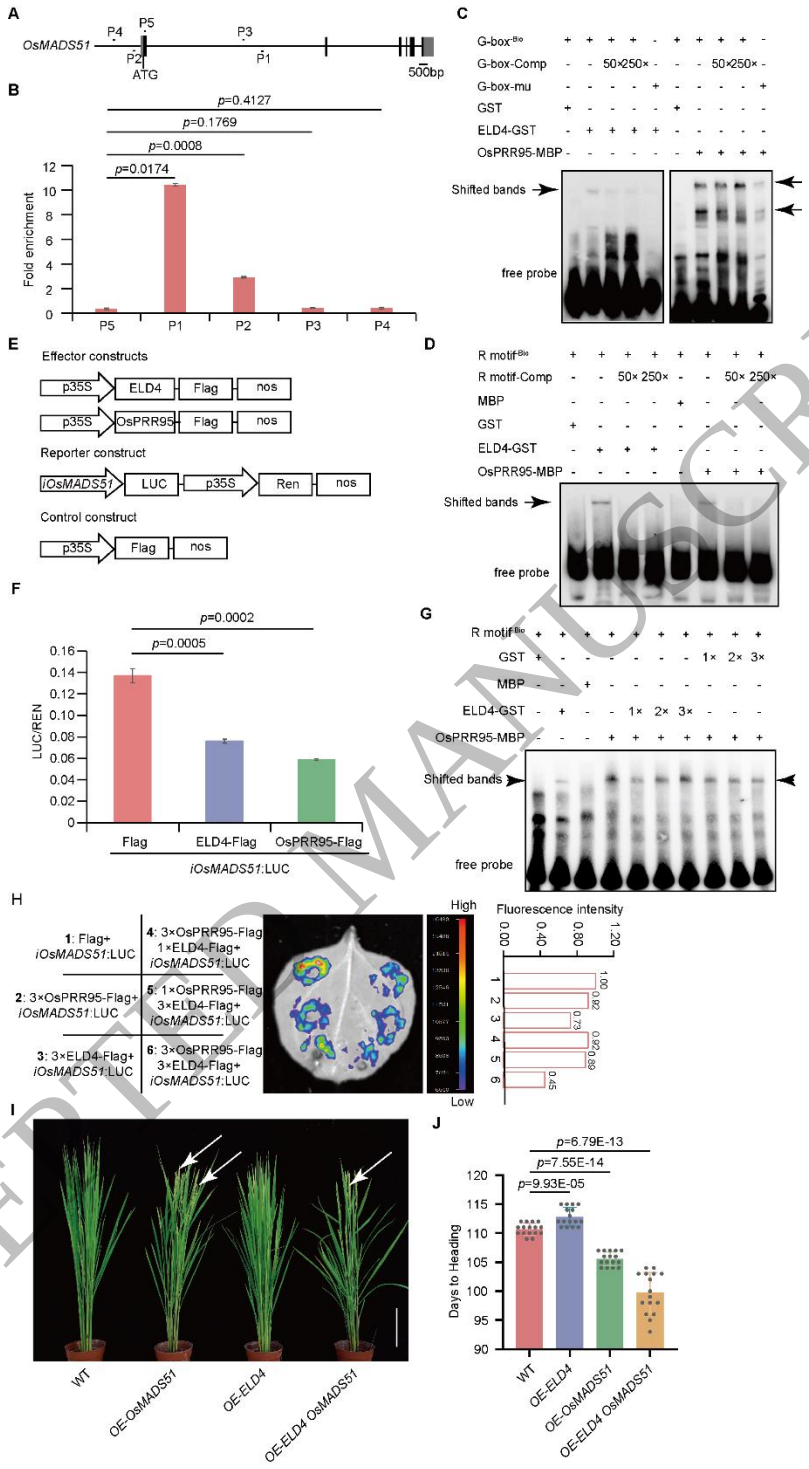

Figure 6
124x229 mm (x DPI)

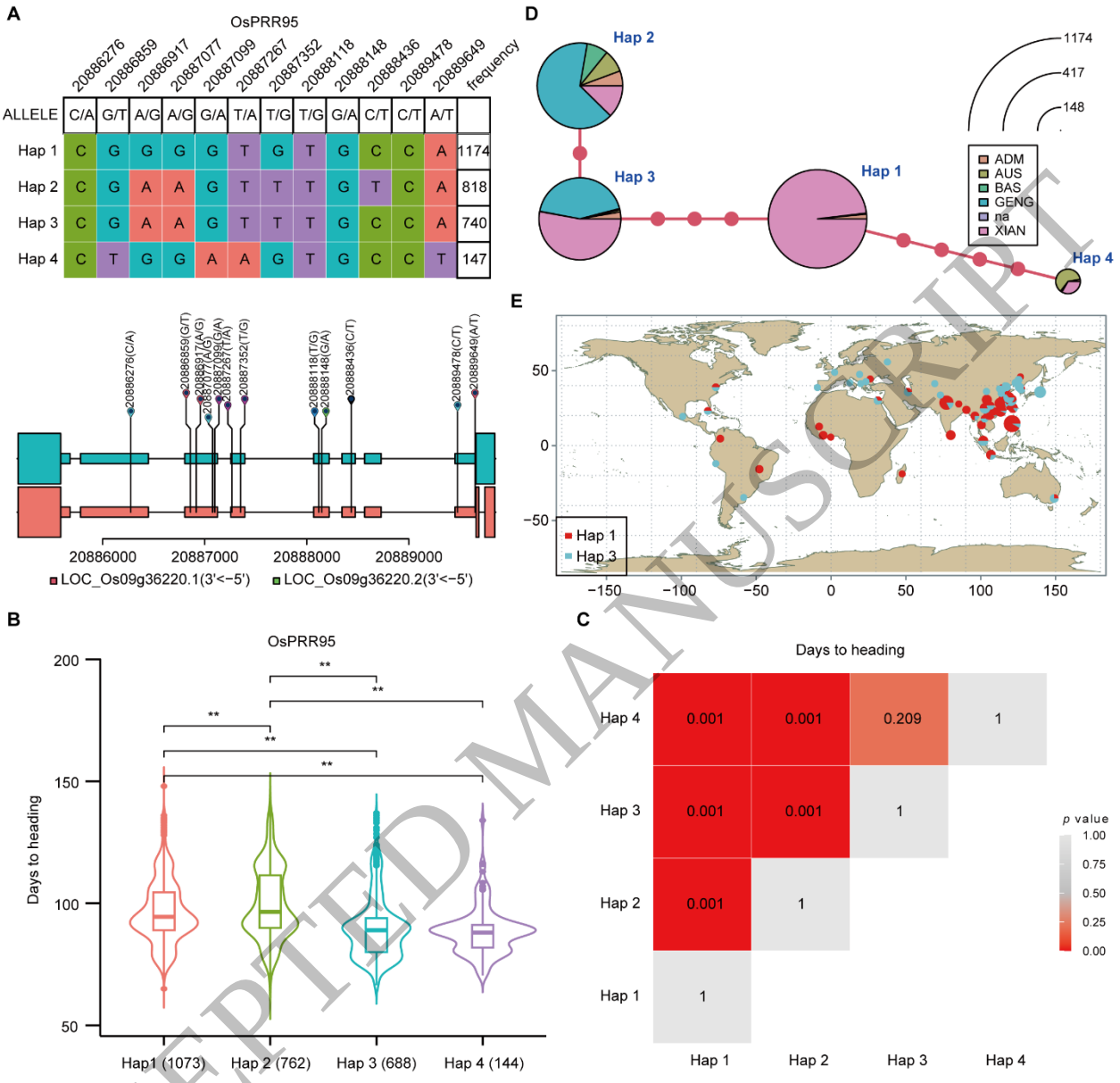

Figure 7
165x158 mm (x DPI)

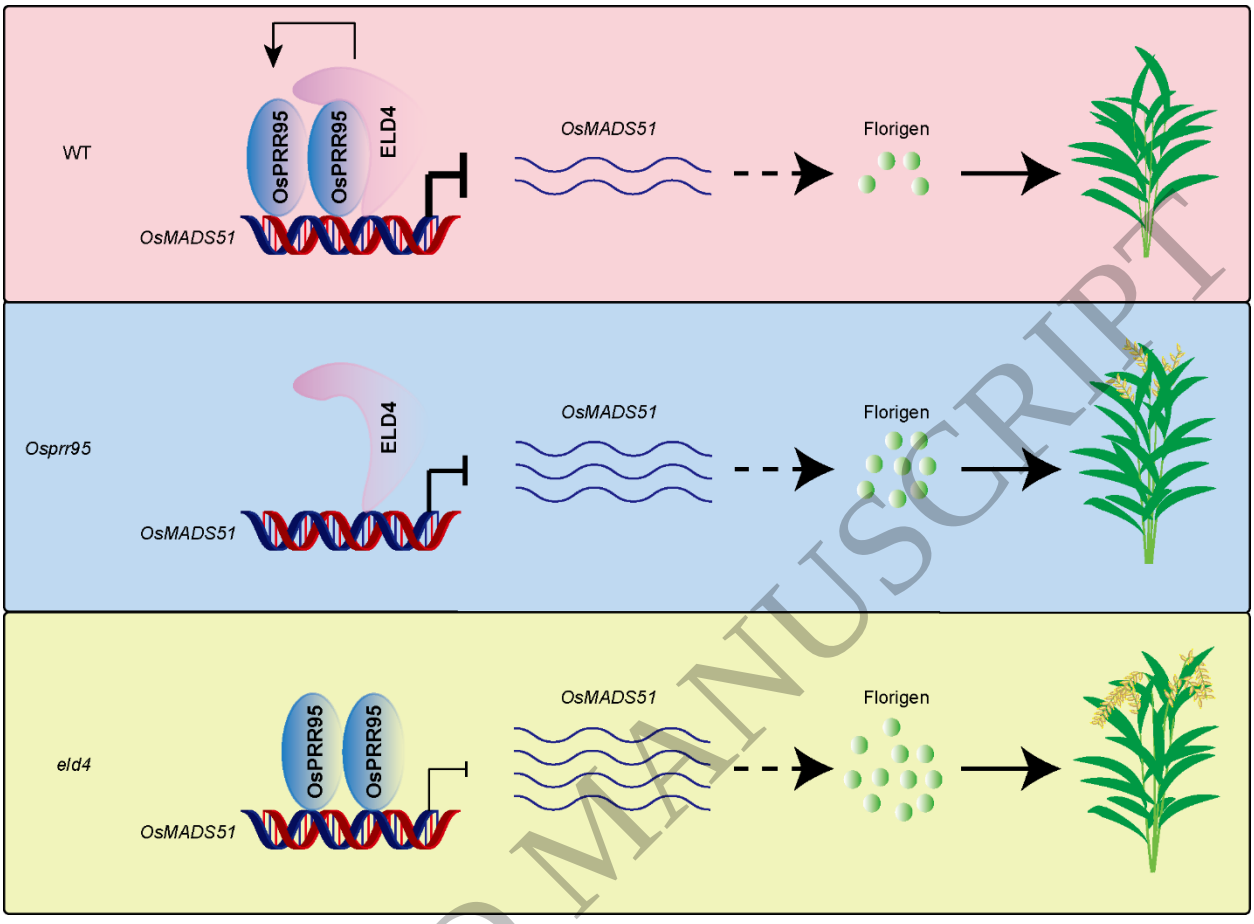

Figure 8
165x120 mm (x DPI)